Advancing the Arctic Methane Permafrost Challenge (AMPAC) With Future Satellite Missions

Annett Bartsch, *Member, IEEE*, Bradley A. Gay, Dirk Schüttemeyer, Edward Malina, Kimberley Miner, Guido Grosse, Andreas Fix, Johanna Tamminen, Hartmut Bösch, Robert J. Parker, Kimmo Rautiainen, Josh Hashemi, and Charles E. Miller

***Abstract*—Permafrost degradation in the Arctic is accelerating and is forecast to enhance greenhouse gas (GHG) emissions from the large permafrost carbon pool. Earth observation has a key role in determining GHG sources and sinks, and multiple current and future missions are useful to track baseline parameters for determining GHG fluxes. NASA and ESA have initialized the Arctic Methane and Permafrost Challenge (AMPAC) as a transatlantic networking action that strives to promote related scientific work and improve observation capabilities. Key variables observable from space include methane concentrations as well as landcover properties to inform process-based models as proxy for sources as well as temperature-related constraints for microbial activity. Upcoming missions are expected to advance these capabilities significantly with increased sampling intervals through future synthetic aperture radar missions and constellations of multiple multispectral sensors. This will allow better representation of seasonality and advance methane source attribution in general. In addition, continuity of current missions, which provide GHG observations, including methane, is crucial. Hyperspectral and superspectral sensors targeting primarily landsurface observation are expected to complement methane retrievals through the identification of emission hotspots. Arctic monitoring also requires active optical instruments for concentration retrieval, a type of instrumentation that is still novel for satellite-based observations. A comprehensive portfolio of hyperspectral, passive microwave, synthetic aperture radar, altimeter and landsurface temperature, and lidar measurements in addition to imaging spectrometers will be available by 2032/2033, at the time of the International Polar Year. This will allow for advanced experiments when also accompanying in situ observations become available.**

***Index Terms*—Arctic, atmospheric observations, Earth observation, land cover, methane, permafrost, remote sensing.**

Received 29 August 2024; revised 21 December 2024; accepted 21 January 2025. Date of publication 5 February 2025; date of current version 28 February 2025. This work was supported in part by the European Space Agency AMPAC-Net project under Grant 4000137912/22/I-DT), in part by the Jet Propulsion Laboratory, California Institute of Technology, through National Aeronautics and Space Administration under Contract 80NM0018D0004. The work of Robert J. Parker was supported in part by the U.K. National Centre for Earth Observation under Grant NE/W004895/1, in part by the Natural Environment Research Council under Grant NE/X019071/1, "U.K. EO Climate Information Service" and in part by the UKRI Future Leaders Fellowship under Grant MR/X033139/1. The work of Annett Bartsch was supported by the European Research Council synergy project Q-Arctic under Grant 951288. *(Corresponding author: Annett Bartsch.)*

Annett Bartsch is with the b.geos GmbH, 2100 Korneuburg, Austria (e-mail: annett.bartsch@bgeos.com).

Bradley A. Gay, Kimberley Miner, Josh Hashemi, and Charles E. Miller are with the NASA Jet Propulsion Laboratory, California Institute of Technology, Pasadena, CA 911093 USA.

Dirk Schüttemeyer is with the ESA ESTEC, 2200 AG Noordwijk, The Netherlands.

Edward Malina is with the ESA ESRIN, 00044 Frascati, Italy.

Guido Grosse is with the Alfred Wegener Institute for Polar and Marine Research, 14473 Potsdam, Germany.

Andreas Fix is with the German Aerospace Center (DLR), 82234 Oberpfaffenhofen, Germany.

Johanna Tamminen and Kimmo Rautiainen are with the Finish Meteorological Institute, 00101 Helsinki, Finland.

Hartmut Bösch is with the Institute of Environmental Physics, University of Bremen, 28359 Bremen, Germany.

Robert J. Parker is with the National Centre for Earth Observation, University of Leicester, LE4 5SP Leicester, U.K.

Digital Object Identifier 10.1109/JSTARS.2025.3538897

I. Introduction

A. Arctic Warming and the Carbon Cycle

GLOBAL climate change is accelerating and already has profound impacts on polar regions and the cryosphere [1]. In particular, over the past decades, the near-surface air temperatures in the Arctic-Boreal Zone (ABZ) have increased 2–4 times faster than the global mean [2]. At the same time, global permafrost temperatures have risen by 0.3–1 °C per decade (e.g., [3], [4]).

Accelerated warming at northern high latitudes is driven by Arctic Amplification (AA) [5], a positive self-reinforcing snow-ice-albedo feedback mechanism. While globally, warming is forced by the increase of atmospheric concentrations of greenhouse gases (GHGs), including carbon dioxide (CO_2), methane (CH_4), and nitrous oxide (N_2O), the enhancement of Arctic warming is caused by a warming-driven loss of snow and ice surfaces, thereby directly decreasing the regional albedo, further amplifying warming and albedo reduction. Additional complex feedback mechanisms include cloud and water vapor feedbacks, changing precipitation patterns, and poleward heat and moisture transport (e.g., [1], [6]), all leading to Arctic warming at an unprecedented pace.

However, the Arctic is not only impacted by the global increase of GHGs and the process of AA, but in turn itself constitutes an integral part of the global carbon cycle with the potential for strong global feedbacks. The Arctic accounts for half of global soil organic carbon despite covering only one quarter of the land surface [7], [8]. Rising ground temperatures and thawing permafrost threaten the stability of large carbon reservoirs, leading to the potential release of latent CO_2 and CH_4 from long-frozen grounds [9], [10], [11] in addition to direct anthropogenic emissions across the Arctic (about one third [12] to 40% [13] of natural emissions depending on the definition of

spatial extent of the Arctic). There is increasing evidence that a changing climate in the modern period has already shifted ABZ ecosystems from net sinks of carbon to net sources, or will do so in the near future [14], [15]. The accelerated transfer of carbon as CO_2 and CH_4 into the atmosphere from thawing permafrost—and its potential impact on future warming—is known as the permafrost carbon feedback (PCF). This self-reinforcing positive feedback may be one of the most critical biogeochemical feedbacks to anthropogenic climate change [7]. For CH_4, both the integrated bottom–up budget and the top–down atmospheric inversion models show consistent sources across Arctic permafrost regions [16], albeit of different magnitudes at 39 and 15 Tg CH_4-C yr-1, respectively. Their uncertainty ranges do not overlap, suggesting that there may be a systematic bias between the methods.

Global wetlands are the single largest, but at the same time least well quantified, natural sources of methane [17]. Indeed, compared to other latitudes, the Arctic has more wetlands and lakes as a direct result of permafrost presence that serves as an aquitard and fosters pooling of surface water [18], [19]. Three out of the five largest wetlands on the globe are located in the Arctic [20], and permafrost regions have the highest density of lakes [21], [22]. In terms of total methane emissions from natural wetlands, the high latitudes rank second behind the tropics [17], [23]. The northern hemisphere permafrost regions have been a methane source for the period 2000–2020 according to bottom-up estimates [24]. Recently, the importance of methane emissions from wetlands not only during the growing but also during shoulder and cold seasons has been highlighted [25], [26], [27], [28]. An expert survey also showed that, globally, most knowledge gaps are related to methane emissions from wetland and freshwater ecosystems (34%) [29].

Fires are another important source of both CO_2 and CH_4 in boreal forests and tundra peatlands which are mostly ignited by lightning strikes. Wildfires are anticipated to become more frequent in the Arctic as a result of warmer and longer summers (e.g., [30]). However, climate models also project increases in annual mean precipitation and a decrease in the number of consecutive dry days in the Arctic, thus future trends in wildfire incidence and severity are unclear [31]. At the same time, since permafrost soils are vulnerable to changes in their thermal regime and reduction of depth of organic soil that overlays and insulates permafrost, wildfires are also significant drivers of permafrost thaw (e.g., [32], [33], [34], [35]). Often, wetlands evolve as permafrost thaws.

The northern high-latitude natural methane sources also overlap with anthropogenic signals from fossil fuel extraction, making the separation of natural versus anthropogenic signals difficult. Reduced sea ice and easier access to remote areas may even increase such activities [36]. Tsuruta et al. [37] showed that increased sampling likely supports the separation of anthropogenic and wetland emissions by satellite data.

GHG emissions from the Arctic may jeopardize global climate goals [38]. However, so far, no conclusive observational evidence of increased methane emission across the Arctic region is provided that may corroborate this hypothesis [39]. The situation is complicated by the fact that the data base from such difficult-to-reach areas is regarded as insufficient.

The Arctic Methane and Permafrost Challenge (AMPAC) has been initiated in order to address these issues. AMPAC is a transatlantic networking action by the National Aeronautics and Space Administration (NASA) and the European Space Agency (ESA). The potential of Earth observation through satellites needs to be exploited and expanded for better understanding of permafrost and active layer processes and resulting methane emissions.

AMPAC aims at the following goals:

1) improve the observation capacity over polar regions by evaluating dedicated campaign activities, by analyzing satellite data, and by identifying satellite retrieval improvements;
2) support the exploitation of the increasing Earth observation (EO) capacity of land surface, cryosphere, biosphere, and atmosphere observations to enhance the scientific understanding of changes in Arctic permafrost regions and methane emissions;
3) bridge the gap between top-down (T-D) and bottom-up (B-U) estimates of methane fluxes in the changing Arctic.

These goals are in line with the requirements of the Global Climate Observing System (GCOS), which listed methane, permafrost, soil carbon and fire as essential climate variables (ECV) which are defined as parameters that critically contribute to the characterization of Earth's climate particularly by means of spaceborne observations. They are also in line with the strategic goals of the Arctic Council concerning monitoring, assessing and highlighting the impacts of climate change in the Arctic and strengthening circumpolar cooperation on climate science and observations.

B. *Important Permafrost and Active Layer Processes*

Quantifying the impacts associated with the degradation of permafrost in the circumpolar Arctic presents a significant scientific challenge. One of the most important impacts, the permafrost-carbon-climate feedback loop, arises from gradual as well as sudden persistent disruptions in the state of permafrost and subsequent complex interactions between newly thawed carbon, shifting ecosystems, and changing climate [40]. Various biotic and abiotic factors contribute to these physical and biogeochemical processes across the tundra and boreal regions. These factors include land surface temperature, precipitation, topography, surface and subsurface water flow, disturbances, tundra shrub encroachment, shift of boreal forest patterns, ungulate migration, and beaver engineering. The northern high latitudes experience amplified release of carbon from thawing soils due to rising temperatures and increased precipitation trends [41]. Although current model projections arbitrarily terminate in 2100 or 2300, it is suggested that anthropogenic-induced warming, combined with enhanced permafrost degradation and soil carbon

decomposition, could trigger positive carbon-climate feedback mechanisms and sustain a warmer and potentially inhospitable state of global climate for hundreds of thousands of years (e.g., [42]).

The permafrost-carbon feedback mechanism could in the future amplify the effects of climate change, triggering destabilization patterns related to permafrost degradation, land-atmosphere coupling thresholds, localized warming, and carbon cycle partitioning [43], [44]. Abrupt thaw initiates ground subsidence, the formation of thermokarst and thermo-erosion features, and the proliferation of emerging wetlands, ponds, and complex hydrological networks, characterized by localized high methane emissions. Permafrost degradation has the potential to generate a significant positive feedback within the climate system and remains a major contributor to uncertainty regarding soil carbon release [44], [45]. Consequently, it is essential to identify and account for confounding factors in model projections in order to comprehend and interpret the response of permafrost carbon to temperature variability [46].

Seasonal dynamics play a crucial role for subsurface freeze and thaw events, with the former occurring when air and surface temperatures fall below 0°C. Despite the prevalence of subzero air temperatures during the cold season, distinct layers of unfrozen subsurface soil may persist between the permafrost below and the frozen active layer above across the Arctic landscape. As recent studies show an increasing regional abundance of these so-called taliks [47], it is crucial to accurately measure and monitor these persistently unfrozen soil zones as their hydrothermal conditions intensify disturbance events, contribute to sustaining near-continuous permafrost degradation, and enable the year-round production and release of GHGs (e.g., methane, carbon dioxide) [48]. This release is evident through soil respiration signals that extend into the cold season.

C. Inferring Methane Emissions

Two methodologies are generally used to infer GHG emissions in order to understand the global carbon budget: The B-U approach assesses emissions by aggregating inventories and using process-oriented models (e.g., biogeochemical models for wetlands or vegetation models). In contrast, the T-D approach is based on atmospheric measurements and inverse modeling in conjunction with an atmospheric transport model. While the latter offers the potential to verify bottom-up emissions with independent measurements, reconciling the two approaches is a significant challenge for accurate budgeting of the major GHGs [16] since both B-U and T-D approaches fail to fully explain recent atmospheric trends [17], [49]. Three prerequisites are required to optimally apply the T-D methodology: First, the atmosphere must be measured at high spatial density and temporal resolution via networks of ground-based stations and aircraft. Second, remote sensing is necessary, from satellites to give global coverage, from the ground to calibrate the satellite data, and from aircraft to bridge the scales. Third, accurate atmospheric transport models are needed, to synthesize the results and convert the concentration measurements to surface flux estimates. B-U requires land observations reflecting the high spatial heterogenity and also temporal dynamics. It is thus a matter of urgency to qualitatively and quantitatively improve our knowledge of the Arctic climate system, understand changes in Arctic permafrost regions and methane emissions and contribute to the accuracy of its prediction by means of improved observation capacities.

D. Remote Sensing Capabilities

Remote sensing provides a range of observation types which have been shown to advance methane flux estimates globally, but challenges remain for Arctic regions. Quantification of fluxes over the entire permafrost domain is currently impeded due to cold season gaps in observations, impacting both in situ and remote sensing measurements. Spatial and temporal gaps and limited representativeness of ground measurements constrain B-U estimates/upscaling [49], [50]. The latter also depends on suitable characterization of permafrost landscapes, specifically wetness gradients, and the identification of land-cover classes with well-quantified flux characteristics. Lake and wetlands classifications need to be clearly separated to avoid double counting in flux upscaling estimates. This has been shown feasible regionally using remotely sensed land-cover (e.g., [51]), but circumpolar implementation at sufficient spatial detail and thematic content is still limited [52]. The fusion of different data sources and expert knowledge such as for example with the Boreal—Arctic Wetland and Lake Dataset (BAWLD) provides a means to overcome some of the limitations [23].

Recent progress has been made in measuring methane concentration through satellites and airborne measurements, but a wide range of issues remain to be solved for high latitude applications (e.g., [40]). Enhanced retrievals and instrumentation could potentially enable consistent coverage across the Arctic, filling the gaps of ground measurements networks through top-down approaches.

An assessment of how much methane ebullition comes from lakes is facilitated through monitoring of ice structure with SAR or optical sensors (e.g., [53], [54]). A further capability of satellite data is the determination of near surface frozen state. Such measurements may improve modeling of flux dynamics in case of sufficient sampling intervals [55].

E. Objectives of This Review

In general, few satellite missions are specifically dedicated to monitor the Arctic. Thus, it is important to analyze to what extent upcoming missions can contribute to the AMPAC goals, and where observational gaps will persist in the near future. The aim of this review is to summarize the potential of upcoming European and NASA missions, to discuss the potential advance beyond the state of the art and to identify remaining gaps.

Remote sensing of the Arctic land surface as well as the atmosphere is crucial, and capabilities need to be further developed. For both, the following sections summarize current

capabilities as well as potential improvements through new approved missions. In addition, parameter specific observation requirements collected by various international initiatives for the purpose of methane monitoring across the Arctic are reviewed.

II. Earth Observation Techniques Supporting Top Down Approaches

For the scope of this study, we categorize respective spaceborne Earth observation techniques into the following two categories:

1) atmospheric methane sensors (SWIR spectrometers, thermal infrared instruments, and lidars);
2) hyperspectral imagers.

The grouping does not quite follow the categories given by a recent paper of [56], in which the authors classify methane sensors as either area flux mappers or point source imagers. Here, we understand methane sensors as instruments that are *specifically designed* to measure GHGs. We differentiate from this category hyperspectral imagers that are typically multipurpose instruments and have a much coarser spectral resolution. At our own discretion, we distinguish spectrometers from hyperspectral imagers according to their spectral resolution and choose as a limit 5 nm. Nevertheless, spaceborne hyperspectral imagers have been shown to be sensitive to high methane concentrations and therefore useful for the retrieval of methane plumes from localized hotspots, and airborne remote sensing of Arctic methane hotspots using hyperspectral imagery indicates that upcoming space-based hyperspectral missions may make contributions to the understanding of Arctic carbon emissions from strong, localized sources [40], [57], [58].

For the scope of this study, we classify atmospheric methane sensors as we understand them into passive shortwave infrared (SWIR) spectrometer, thermal infrared (TIR) sensors, and active (lidar) optical remote sensing instruments, which all typically provide XCH_4, or more generally, XGHG, as the measured quantity. XCH_4 is the weighted average of the methane dry-air volume mixing ratio along the probed column. SWIR spectrometers collect backscattered solar radiation mainly from the ground, which has been modified by absorption from atmospheric gases. Based on absorption spectroscopy, the depth of those absorption lines in the measured spectra can be interpreted as column gas concentrations in the atmosphere. TIR spectrometers are also based on absorption spectroscopy but in general make use of the thermal radiation emitted from the Earth. Modern spectrometer systems often (but not exclusively) provide imaging capabilities. In contrast to passive remote sensors, lidars have their own light source and can measure atmospheric methane, using the differential absorption of a pair of spectrally closely adjacent laser lines [59]. Thus, lidars are independent of sunlight, i.e., seasonality or time of the day. Moreover, lidars are much less affected by thin clouds or aerosol layers, such as from wildfires, which are common in the Arctic.

Thermal infrared instruments are included as they are able to provide valuable methane information throughout day and night and all seasons, despite the fact that they have their highest sensitivity in the free to upper troposphere and lack information from layers close to the ground. On the other hand, we exclude missions, that due to their orbit, do not reach Arctic latitudes, e.g., from the International Space Station (ISS) as the platform, like EMIT [60].

A. SWIR Spectrometers

The first satellite instrument that could measure methane in this way was SCIAMACHY, a German-Dutch-Belgian instrument on the ESA ENVISAT satellite from 2002 to 2012 [61]. It was followed by the Thermal and Near-Infrared Sensor for Carbon Observation (TANSO), a Fourier-Transform-Spectrometer, onboard the Japanese JAXA/NIES/MOE Greenhouse gases Observing Satellite (GOSAT) [62], which has been in operation since 2009, followed by its successor in 2018, GOSAT-2 [63]. GOSAT-1 and -2 also feature a thermal infrared channel [64] (see below). In 2017, the Tropospheric Monitoring Instrument (TROPOMI) onboard the Copernicus Sentinel-5 Precursor (S5P) satellite complemented the suite of methane monitoring satellites. TROPOMI has improved CH_4 mapping by providing much denser coverage than previous missions. SWIR sensors can provide (although to a limited temporal extent—late winter) cold season measurements. Recent TROPOMI retrieval algorithm updates have improved both the quality and coverage of the observations in high northern latitudes [65]. Nongrowing season Arctic CH_4 fluxes account for approximately 50% of annual emissions [26], [28].

Apart from the above listed purely scientific missions, GHGSat Inc. started to launch their commercial fleet of methane sensing instruments in 2016. At the time of writing this manuscript as many as 9 satellites were part of the constellation that mainly delivers high-resolution local image data to identify point sources of methane (CH_4) emissions to individual facilities to serve the need of the oil and gas (e.g., [66]), mining, waste management, and agricultural industries. The same holds true for the recently (2024) launched MethaneSAT mission, but with a somewhat wider coverage and coarser spatial resolution. In practice, the combination of high spatial resolution of GHGSat (or Sentinel-2, PRISMA, see below) and frequent sampling of TROPOMI has turned out to be efficient for identifying local emission hotspots (e.g., [67]).

B. Thermal Infrared Instruments

IASI is a series of three identical instruments built in cooperation between CNES and EUMETSAT for operation on EUMETSAT's MetOp satellites. They were launched in 2006 (IASI-A), 2012 (IASI-B), and 2018 (IASI-C). IASI measures more than 25 atmospheric components including temperature and humidity, along with many atmospheric gases including methane. However, due to its measurement principle using thermal IR, IASI has very low sensitivity to surface methane. The vast majority of the information content is limited to the upper troposphere (approx. 5–12 km, so called midtropospheric column) [68], so IASI is only partially suitable for the detection of sources located on the ground. Nevertheless, IASI products (together with GOSAT) are the only satellite products that are currently

ingested into the COPERNICUS Atmospheric Monitoring System (CAMS) global GHGs reanalysis [69]. In addition, IASI data (together with AIRS) were used in a study that observed methane anomalies over the Arctic seas peaking in winter and thought to originate from transport from the seafloor [70]. The next generation of IASI instruments, IASI-NG [71] will fly on EUMETSAT's METOP-SG satellites (see below).

The Cross-Track Infrared Sounder (CrIS), is a series of TIR instruments, with channels sensitive to methane [72]. CrIS is on the Suomi National Polar-orbiting Partnership (NPP) satellite and has been operational since 28 October 2011 [73]. An additional copy of CrIS is also aboard NOAA's Joint Polar Satellite System (JPSS) NOAA-20, launched in 2017; and is planned to be included on a series of follow-on satellites over the coming years (NOAA-21, NOAA-22). CrIS is a nadir viewing Fourier transform spectrometer (FTS) that measures TIR radiances and provides daily global measurements of midtroposheric methane columns with a swath width of 2300 km. The wide spectral range and high spatial sampling allows CrIS to retrieve a range of atmospheric composition products beyond methane, such as carbon monoxide, ozone, and many others.

C. Lidars

A very promising technology enabling measurements to be made globally in all seasons at all latitudes, both during daylight and nighttime, is light detection and ranging (lidar). As an active method using laser radiation, lidar observations do not generally require reflected sunlight. Hence, lidar holds particular appeal for Arctic measurements. The main data product is the column-weighted dry-air mixing ratios (XGHG), which can be measured using the integrated-path-differential-absorption lidar technique (IPDA) [74].

Several mission ideas such as Active Sensing of CO2 Emissions over Nights, Days, and Seasons (ASCENDS), [75] by NASA, or Advanced Space Carbon and climate Observation of Planet Earth (A-SCOPE) [76]) by ESA, have been proposed to measure carbon dioxide columns with lidar but were finally not selected for launch. However, based on that heritage, China launched the Atmospheric Environment Monitoring Satellite (AEMS) carrying the Aerosol and Carbon Detection lidar (ACDL) in 2022 [77], [78] which could serve as a blueprint for a methane lidar specifically to show the expected benefit for Arctic measurements. The French–German MERLIN mission to be launched in the 2029 time-frame likely will be the first lidar mission to measure XCH_4 globally from space [59].

D. Hyperspectral Imagers

Significant advancements in image processing techniques have facilitated the identification and analysis of methane and carbon dioxide anomalies, leading to the creation of valuable benchmark data for validation and scaling purposes. Despite the challenges involved, the utilization of near-infrared (NIR) and shortwave infrared (SWIR) signals has been continuously improved through the implementation of sophisticated methodologies and calibration updates, including imaging software, filtering techniques, and inversion modeling. Additionally, the use of AVIRIS instruments (Airborne Visible InfraRed Imaging Spectrometer; airborne) has greatly contributed to studies related to ecosystem functioning, biogeochemical cycling, disturbance mapping, and geomorphological research. Moreover, considerable technological progress has been made in extracting gaseous signatures, particularly GHGs such as carbon dioxide and methane, by analyzing the reflected solar radiance emitted by plumes and seepage. For example, the combination of segmentation and classification techniques has greatly enhanced the ability to detect and differentiate true point sources of methane from false positive anomalies across large areas [79]. The SWIR signatures have been evaluated by comparing them to in situ reference measurements and laboratory spectra, specifically targeting the methane window within the range of 365–405 and 2200–2400 nm, with a sampling interval of 5 nm and a resolution of 0.3–4.0 m [80].

There has been recent progress through the use of imaging spectroscopy. Methane emission hotspots have been identified with the 5 m provided by AVIRIS [57], [81]. In a regional study, methane emissions in the Arctic have been found to demonstrate a power law relationship with the distance from standing water, highlighting the importance of characterizing the associated distribution patterns [81]. Saturated conditions and the resulting concentration and prevalence of methane plumes exhibit a gradient of 40–300 m, with a higher number of plumes and greater methane concentrations observed nearer to water bodies and riverine networks [82]. These findings contribute to the understanding and refinement of spatial scaling efforts, enabling better quantification of the connections between GHG emissions and subsurface ground ice (i.e., the influence of soil moisture content on active layer thickness).

III. Land Surface Monitoring Facilitating Bottom up Approaches

Key observable of the land surface in the context of methane and permafrost research are land cover as proxy for carbon storage (e.g., [83], [84]), land-atmosphere exchange (e.g., [17], [51]) and surface temperature and state as proxy for subground conditions including its temporal dynamics for characterizing the switch of microbial activity and plant functions (e.g., [55]). Fluxes are up-scaled based on wetland and lake characteristics (distribution, type, dynamics, lake ice properties, etc.).

Primary variables for which dynamics are required are:

- wetland type and open water distribution;
- open water seasonal dynamics;
- soil moisture dynamics.

Temperature-related variables of added value include:

- land surface freeze/thaw state;
- land surface temperature;
- active layer dynamics.

For the determination of methane processes during the frozen period, applicable in specific regions is:

- lake ice structure (ebullition proxy).

Of further relevance regarding carbon sources are:

- soil carbon; and
- fire occurrence.

A. Primary Variables

In the past, static snapshots were used to produce global land cover maps from satellite observations, often with limited class diversity for the Arctic permafrost regions [85], [86]. Few datasets focused specifically on the Arctic and its ecological and functional diversity and many were limited to specific subregions such as the tundra biome (CAVM - Circumarctic Vegetation Map, [87], CAWASAR - Circumarctic wetland dataset based on ENVISAT ASAR [88]) or geographic areas, such as the Lena Delta [51], [89], Usa basin [90], or the Barrow Peninsula [91]. Landcover maps based on satellites were initially designed for purposes such as habitat and general vegetation mapping [85]. However, such landcover maps have also been investigated at local to regional scale in order to identify sources of carbon (soil organic carbon, wetland distribution, lakes) (e.g., [51], [92]). Covered areas are usually comparably small in case of upscaling dedicated efforts as based on very high spatial resolution data (e.g., [93]). The focus has been, in general, on mapping areas with potentially high emissions, rather than identification of gradients, spatially and temporally. Multiple sources for landcover information have been fused for a first circumpolar representation including the boreal domain in the Boreal-Arctic Wetland and Lake Dataset (BAWLD, $0.5°$) [23].

An important aspect where higher resolution remote sensing will help with enhancing methane emission upscaling is the differentiation between wetland and lake types in order to identify emission hotspots, i.e., identifying wetland landcover classes that are small in spatial coverage but have disproportionate impact on landscape-scale emissions, as well as to avoid double-counting of wetland and lake emission sources quantified in field measurements upon upscaling. In northern wetlands, for example, fens are much higher methane emitters than bogs, but often cover a significantly smaller proportion of the landscape in a study region. Additionally, specific small water bodies such as thermokarst or beaver ponds have been identified as especially large methane sources, while larger lakes often have much smaller emissions [94]. Hence a proper lake detection and classification is important and the remotely sensed tracking of their growth, stability, and drainage or drying is critical to capture the dynamic transitions between wetlands and lakes in the rapidly changing permafrost region [10], [95], [96], [97]. An initial circumpolar attempt at lake methane emission upscaling took different lake classes and lake seasonality derived from remote sensing with higher detail into account [98].

One of the main issues is that there is currently no remote sensing-based circumpolar land cover map with sufficient spatial detail and thematic content available to support upscaling of soil properties and fluxes for the entire Arctic [85], [86]. The technical feasibility through fusion of optical and SAR data has been, however, demonstrated with ESA GlobPermafrost prototypes that fused Sentinel-1 and Sentinel-2 data at 20 m resolution (scheme applied in [99] and [100]). The result is a static map, as there is a limitation through use of Sentinel-2 due to frequent cloudy condition in the Arctic and short growing season [52]. While this approach serves the needs for permafrost model parameterization, it does not fully address the needs for upscaling of methane fluxes, specifically variations of waterlogged conditions across the seasons and from year to year.

Over recent years, mapping land cover dynamics (trends, disturbances) at high temporal resolution became more and more feasible to understand changes in permafrost region land cover characteristics [95], [101], [102] and could provide highly relevant continuous land cover time series for quantifying longterm changes in methane production and emission in a rapidly warming region [103], [104]. A key parameter for methane production in permafrost landscapes is the representation of the heterogeneity of tundra landscapes, specifically the coverage of wet versus dry areas and their dynamics over time [105]. In order to address wetting and drying processes, both open water fraction change and soil moisture-related information are essential.

While mostly optical/multispectral data (especially Landsat) have been used to identify wetland related landcover in Arctic environments so far, SAR can provide valuable wetland information. For example, With better availability of *C*-band SAR over larger regions through ENVISAT ASAR, both a regional (75 m, wide swath mode, [106]) and a circumpolar (500 m, global monitoring mode, [88], [107]) mapping of wetlands were achieved.

The current global assessment of the methane budget [17] integrates global coarse resolution wetland dynamics, while for the Arctic static information on landcover as a proxy for soil carbon (separation of mineral and organic soils) is derived from the CAWASAR [88], [107]. This dataset is based on the past ENVISAT mission (2002–2012), which included a *C*-band SAR sensor with a so-called global monitoring mode. This mode was activated when no other data types were acquired. It resulted in a so far unique dataset with circumpolar coverage. This has not been achieved with other SAR missions (including the ENVISAT ASAR successor Sentinel-1) until now due to limitations in the respective acquisition strategies across the Arctic. A further advantage of the ENVISAT ASAR Global monitoring mode was the consistent availability of HH polarization, which provides a representation of the soil surface in regions with limited vegetation coverage such as Arctic tundra. *L*-band SAR provides better representation of soil and wetland conditions (e.g., [106]), but is currently not consistently available for the Arctic. This will change in early 2025 with the launch of the NASA-ISRO synthetic aperture radar (NISAR) which will deliver *L*-band imagery across the pan-Arctic.

Temporal dynamics based on satellite records have so far only been considered with respect to inundation, which can be derived at a coarse scale (fraction) based on passive microwave observations (e.g., [108]) and at medium resolution using indices from optical data [95].

A so far slower advance in product development than for wetland dynamics can be observed for soil wetting and drying. In the Arctic, the landscape heterogeneity and especially the occurrence of lakes, has so far been a major limiting factor for retrieval of near surface soil moisture time series using microwaves (e.g., for SMAP [109], and Metop ASCAT [110], SMAP & SMOS [111]). Approaches used for global services are of limited applicability due to lower spatial resolution and further

Arctic-specific factors. Differences in spatial detail impact the performance of models used for methane flux estimation [112]. In addition, general assumptions of mineral soil structure in retrieval algorithms rather than the highly organic Arctic soil properties are fairly common constraints to more effective soil moisture retrievals [113]. Accordingly, retrieval algorithms will need to be revised, for example, considering more realistic soil dielectric models and properties in permafrost soils with frequent freezing and thawing, high organic matter content, and significant ground ice content.

Local InSAR subsidence patterns have also been found to represent wetness gradients (e.g., [99], [114], [115]). This could be found for all available wavelengths including *C*-band for the Copernicus Sentinel-1 mission. Product development is, however, lacking to date. In addition, the feasibility for implementation over large regions such as the Arctic is currently limited.

B. Surface Temperature Related Variables

Landsurface temperature obtained through thermal sensors, specifically MODIS, has been key for a first assessment of permafrost state globally, and its dynamics for the northern hemisphere [86]. It could be shown that the Northern hemisphere permafrost is continuously warming across all permafrost regions based on annual ground temperature retrieval by [116]. Data were gap-filled (due to frequent cloud cover) with reanalyses data and ingested into a model (CryoGRID, [117]) for representing heat transfer. If available at sufficient spatial detail (1 km or better), snow parameters, especially SWE, can be considered in the modeling.

The use of comparably coarse resolution passive and/or active microwave observations provide a solution regarding cloud cover, but only surface state can be derived. Sensors suitable for surface state retrieval include radiometers, radar and radio-occultation techniques. Freeze/thaw state can be determined to quantify growing season length and to analyse related fluxes [55], but this information is confined to the surface. The consideration of active layer (upper soil below the top 5 cm) freeze-up patterns is also needed to fully account for microbial activity. Satellite missions for which freeze/thaw products are available provide measurements from passive microwave sensors (SMAP, SMOS, and AMSR-E and SSMI products of MEaSUREs, [118], [119], [120]). An experimental product is also available from radar (Metop ASCAT—Advanced Scatterometer) based on [121]. The unfrozen period length detected through *C*-band radar differs considerable from MEaSUREs [122] which results from the shorter wavelength of the passive microwave observations in case of SSMI. An experimental operational FT product at 1 km spatial resolution for boreal forests based on Sentinel-1 SAR data [123], [124] is currently only available for Finland. It is planned to be extended to other regions in the future. An optimized product targeting flux studies in permafrost regions does not exist to date. Issues arise also in mountainous terrain [125], [126] and areas with high water fractions as typical for Arctic tundra [100] due to the comparably coarse spatial resolution.

C. Lake Ice Monitoring

Methane ebullition from lakes in wintertime has been addressed through monitoring of lake ice properties with SAR data [127]. They are interpreted in two ways. First, bubbles in the ice are inferred from radar backscatter under the assumption that ice structure is having an impact on the signal return. It could be shown that the amount of trapped methane can be estimated [127]. Second, strong, constant ebullition from major seeps prevents ice formation and results in open water holes, which can be identified with VHR data as well as medium resolution SAR derived ice structure (and thus backscatter) is impacted in the surrounding of the holes [54], [128]. Relevant information can be obtained from *C*-band as well as *L*-band SAR [128], [129].

IV. Approved Future Missions

Planned satellite missions of NASA, NOAA, ESA, DLR, and CNES in advanced stage (approved; Table I) are expected to improve the assessment of landsurface hydrology as well as methane concentration in the atmosphere. The majority are active and passive microwave missions, but also advancements on thermal and hyperspectral observations are expected to be beneficial for the investigation of permafrost regions. More information about the orbit characteristics of the satellites is provided in Tables IV and V.

A. European Future Missions

The Copernicus Imaging Microwave Radiometer (CIMR) mission employs multifrequency imaging microwave radiometers to provide day and night observations of primarily sea ice. Spatial resolution (≈5 km), temporal resolution (subdaily) and geophysical accuracy are improved through use of a conically scanning radiometer. Land surface temperature and surface state products are, however, also foreseen. The subdaily resolution will enable monitoring beyond the state of the art. The errors on these type of LSTs are slightly larger than for their infrared counter parts, but the estimates are available ∼90% of the time (compared to less than ∼40% of the time with the infrared estimates). The retrieval requires a priori estimates of vegetation coverage. The planned snow products, which are enabled through the whole suite of L- to Ka-band data, are expected to be of benefit for permafrost modeling.

The Copernicus Polar Ice and Snow Topography Altimeter (CRISTAL) mission will provide enhanced measurements of land ice elevation and sea ice thickness. But while elevation change is a key parameter for the detection of permafrost degradation, the changes are mostly too subtle to be captured through altimeter missions [130]. However, landsurface hydrology change, which results in lake water level change could be detected for larger lakes with secondary products of CRISTAL.

The Copernicus synthetic aperture Radar Observing System for Europe in *L*-band) (ROSE-L) mission [131] is responding to the requirements expressed by both the land monitoring and the emergency management services. Its target applications are soil moisture, crop type discrimination, forest type/forest cover

TABLE I
APPROVED FUTURE US AND EUROPEAN MISSIONS (NASA, NOAA, USGS, ESA, EUMETSAT, DLR, CNES, UKSA) AND EXPECTED ADDED VALUE FOR QUANTIFICATION OF ARCTIC PERMAFROST METHANE FLUXES

Mission	Type	Primary target	Launch	Agency (program)	Relevant products	Added value comment
Metop-SG A (Sentinel-5)	imaging spectrometer	trace gases	2025	ESA EUMETSAT EC (Sentinel)	CH_4	7 km, Continuation of TROPOMI (Sentinel-5P)
Metop-SG A (IASI-NG)	imaging spectrometer	trace gases	2025	EUMETSAT, DLR , EC, CNES, ESA	CH_4	limited - 45 km, but continuation mission
CO2M	imaging spectrometer	trace gases	2026	ESA EUMETSAT EC (Sentinel)	CH_4	2 km, 250 km swath
JPSS3/4 (CrIS)	Cross-Track Infrared Sounder	temperature/ humidity sounding, coarse ozone profile , and total-column green-house gases	cont. to 2039	EUMETSAT, NOAA, NASA	CH_4	limited - 50 km field of regard, but continuation mission
MERLIN	(IPDA) lidar	trace gases	2029	CNES, DLR	CH_4	all seasons, 100 m lidar footprint
TANGO	imaging spectrometer	trace gases	2027	ESA (Scout)	CH_4	limited - 300 m spatial resolution, but focus on industrial targets foreseen
CHIME	hyperspectral	landcover, agriculture	2029	ESA EUMETSAT EC (Sentinel)	TOA and BOA	>200 bands, 30 m, two satellites, advance in wetland monitoring, potential for methane hotspots identification
LandsatNext	superspectral	landcover	2030	NASA, USGS	TOA and BOA	26 bands, 10-60m, advance in wetland monitoring
NISAR	synthetic aperture radar	deformation, inundation, etc	2024	NASA/ISRO	L1 to L4, specifically soil moisture and land inundation	first time regular circumpolar coverage for SAR expected
HydroGNSS	GNSS reflectometry (bi-static radar)	soils	2024	ESA, UKSA (Scout)	soil moisture, freeze/thaw state, inundation	5-7 km, added value to be clarified
CRISTAL	radar altimeter	land and sea ice	2028	ESA EUMETSAT EC (Sentinel)	tbd	limited to detection of extreme cases of topography change
HARMONY	passive synthetic aperture radar	Small scale motion and deformation	2029	ESA (Earth Explorer)	tbd	abrupt thaw feature monitoring
ROSE-L	synthetic aperture radar	agriculture and emergency management	2029	ESA EUMETSAT EC (Sentinel)	tbd	advance for permafrost wetland monitoring, consistent, regular coverage crucial
CIMR	passive microwave	sea ice	2029	ESA EUMETSAT EC (Sentinel)	snow area, SWE, freeze/thaw state, landsurface temperature	sub-daily, 5 km, better shoulder season analyses specifically in relation to fluxes
LSTM	thermal	landsurface temperature	2029	ESA EUMETSAT EC (Sentinel)	landsurface temperature	better spatial resolution, 37-50 m, better temporal coverage through two satellites
JPSS3/4 (VIIRS)	Visible Infrared Imaging Radiometer	hurricanes, fires, smoke, and atmospheric aerosols	cont. to 2039	EUMETSAT, NOAA, NASA	landsurface temperature	limited - 750 m spatial resolution only at Nadir
HARMONY	multibeam thermal-infrared	Clouds and sea surface temperature	2029	ESA (Earth Explorer)	tbd	land monitoring not targeted

(in support to biomass estimation), food security, and precision farming. General added value is expected through synergetic and complementary observations with *C*-band and *X*-band SAR systems. This is expected to apply also for permafrost wetland characterization. The use of *L*-band will also be of benefit for degradation monitoring. It is expected that it will provide continuity for observations from PALSAR and PALSAR-2 and future acquisitions from NISAR. A consistent coverage for permafrost regions will be, however, crucial.

The main level 2 products of the Copernicus Land Surface Temperature Monitoring (LSTM) mission will be land surface temperature and land surface emissivity [132]. Higher spatial resolution would be the main benefit for permafrost-related modeling and monitoring. This also includes lake surface

temperature monitoring, which has so far been limited to larger lakes only across the Arctic (e.g., [133]), neglecting the vast majority of lakes, and specifically those of relevance for methane emissions. The targeted 37–50 m, with acquisitions coming from eventually two satellites are expected to advance permafrost modeling and thaw lake monitoring.

The Copernicus Hyperspectral Imaging Mission for the Environment (CHIME) mission [134] aims to augment the Copernicus space component with precise spectroscopic measurements to derive quantitative surface characteristics. Synergistic acquisitions with Sentinel-2 are foreseen, including a target resolution of 20 m for combined use. Hyperspectral data have been shown to allow better separation between tundra species [135] and will thus be of benefit for specifically wetland monitoring, but the targeted spatial resolution will pose a limit for applications due to Arctic landscape heterogeneity. A combined use with ROSE-L may allow for better characterization of wetland seasonality and specifically permanently wet lake margins which play a crucial role for methane emissions. The potential for methane retrieval from hyperspectral data has also been demonstrated for methane concentrations, specifically identifying hotspots for natural emissions using airborne data [57] and industrial hot spots using satellite observations (Sentinel-2, [58]).

The Copernicus Anthropogenic CO_2 Monitoring (CO2M) mission [136], [137] employs imaging spectrometry to monitor man-made CO_2 and CH_4 emissions and overall CO_2 and CH_4 budget at country and regional/megacity scales and assess the effectiveness of the relevant emissions reduction commitments. This requires a capability to provide accurate and consistent quantification of anthropogenic CO_2 and CH_4 emission and their trends.

HydroGNSS is a new ESA Scout mission which targets four hydrological variables: surface soil moisture, inundation (focusing on wetlands), seasonal freeze, and thaw state (focusing on permafrost areas), and above-ground biomass [138]. The launch is expected in 2025. Two identical satellites will use a technique called Global Navigation Satellite System (GNSS) reflectometry. It will collect *L*-band GNSS signals (dual polarization and dual frequency) with a theoretical spatial resolution of 5–7 km. Through the use of two satellites and a low Earth orbit (LEO), a temporal resolution of 15 days can be achieved. Retrieval of surface state [139], [140] and wetlands [141] has been shown feasible. However, for the high latitude areas, there should be data available more frequently. The spatio-temporal setup is less beneficial than upcoming *L*-band SAR missions for monitoring of wetland dynamics. The advantage of the dual frequency remains to be assessed. Added value might be achieved through combined use with SAR missions.

The Harmony concept [142] comprises two identical *C*-band satellites that fly in a configurable formation alongside a Copernicus Sentinel-1 satellite, which serves as an illuminator. Each Harmony satellite is designed to carry a receive-only SAR instrument as its main payload. It is an ESA Earth Explorer mission, which will be launched in 2029. The constellation enables new observation capabilities, revealing finer details and insights of the Earth's surface including ground motion [143]. It will provide advanced capabilities for monitoring permafrost abrupt thaw features such as thaw slumps. The 12 d repeat cycle will aid in the process of understanding the development of such erosion features, which are triggered by heat waves [144] and result in land cover change and carbon transport [145]. The identification of subtle subsidence patterns provides insight into active layer dynamics on seasonal scale and ground ice loss when considering long-term trends. Harmony will also carry a thermal infrared (TIR, 1 km) instrument, but it targets vertically resolved cloud movements [143]. When clouds are not present, the instrument will measure the ocean surface temperature. A prototype of this instrument will be available from the EPS-Sterna microsatellite constellation mission (Arctic Weather Satellite).

TABLE II
SPECIFICATIONS OF THE LEVEL-2 METHANE PRODUCT OF MERLIN [59]

Systematic error	3 ppb
Random error	22 ppb
Spatial resolution	0.1 x 50 km
Spatial coverage	global
Vertical resolution	total column

Following Sentinel-5p with the TROPOMI instrument, the Sentinel-5 mission consists of a single instrument which is a UV-VIS-NIR-SWIR spectrometer. It will be part of the MetOp-SG A satellites which are operated by EUMETSAT as part of the EUMETSAT polar system second generation (EPS-SG) system. Sentinel-5 is focused on air quality and composition-climate interaction. The level-2 product suite includes CH_4 total column concentration with 7 km sampling resolution and daily global coverage. Compared to Sentinel-5P, Sentinel-5 will fly in the morning orbit. Interestingly, the same platform will also host the IASI-NG instrument. It would be important to analyze if joint analysis of these two instruments, with different vertical sensitivities on methane profile, could improve monitoring tropospheric methane columns and allow improved emission quantification [146].

Twin Anthropogenic Greenhouse Gas Observers (TANGO) [147] has been selected as a new ESA Scout mission. It will complement measurements of methane and nitrogen dioxide from the current Copernicus Sentinel-5P mission and the upcoming CO2M mission. TANGO will focus on predefined areas, specifically known large industrial facilities and power plants. They will be monitored every four days. It will deliver high-resolution images of emission plumes as well as the surrounding pollution, with sufficient accuracy to determine industrial emissions with a single observation. The instrument has a field of view of 30×30 km^2 at a spatial resolution of 300 m.

The Methane Remote Sensing LIdar Mission (MERLIN) under the joint auspices of the German and French Space Agencies, DLR and CNES, is currently under development [148] to measure XCH_4 with a projected launch date in early 2029 (for specifications see Table II). The main scientific objective of MERLIN is the delivery of weighted atmospheric columns of methane dry-air mole fractions for all latitudes throughout the

year with systematic errors small enough (<3 ppb) to significantly improve our knowledge of methane sources from global to regional scales, with emphasis on poorly accessible regions such as the high latitudes. MERLIN is based on an integrated path differential absorption nadir-viewing lidar (IPDA) [59]. The IPDA technique relies on differential absorption lidar measurements using a pulsed laser emitting at two wavelengths around the methane doublet at 1.645 μm, one wavelength accurately locked on a spectral feature of the methane absorption line, and the other wavelength, almost free from absorption, used as a reference. The differential approach, the size of the laser spot ($\sim$100 m at the surface along the track), and the selective sampling guarantee low systematic errors (target <3 ppb) and measurements in broken-cloud conditions, with almost no contamination by aerosol or water vapor. The expected random errors at a 50-km resolution (baseline averaging length) are not particularly small compared to existing or planned missions [59]. But, the contribution of the random errors on flux estimation on a regional scale remains limited, as the latter is dominated by the impact of systematic errors. It was shown that, on average, MERLIN should better constrain the methane budget for the high latitudes than current and planned passive GHG missions [149].

B. NASA/NOAA Future Missions

Approved NASA/NOAA missions cover both land surface and atmosphere monitoring. While the 2017 National Academies' Decadal Survey, which identifies needs for NASA missions, prioritized terrestrial ecosystem, and near-coastal dynamics globally, research since continues to emphasize the critical role of the Poles in driving climate. Missions in development as part of the NASA Earth System Observatory will capture changes in the near Arctic and coastal-land interface. These include the Surface Biology and Geology (SBG) thermal and visible shortwave instruments, and the mass change measuring system that is a follow-on the gravity recovery and climate experiment (GRACE).

Current NASA missions often target the midlatitudes in sun-synchronous orbits, but recent collaborations with partners have allowed for greater satellite breadth and coverage. Starting in 1996, with the launch of the POLAR satellite, coverage of the poles yielded novel information on the and ionosphere. Since then, ground and airborne campaigns have visualized the surface at greater resolution over time. In 2022, NOAA and NASA launched a joint mission for observations, the Joint Polar Satellite System (JPSS). JPSS is a suite of satellites and instruments, with JPSS-3 and -4 launching in the next few years. The constellation in its entirety contains five satellites when complete. The mission is foreseen to continue until 2039 with subsequent satellite launches.

The JPSS satellite constellation carries a diversity of instruments [150], [151], including Advanced Technology Microwave Sounder (ATMS), the Ozone Mapping and Profiler Suite (OMPS), the Cross-track Infrared Sounder (CrIS), and the Visible Infrared Imaging Radiometer Suite (VIIRS). This is in addition to onboard monitoring of the Earth energy budget. Together, these instruments will monitor a diversity of Arctic and near-Arctic dynamics, including land and sea surface temperatures, snow and ice cover, fire, rainfall rates, atmospheric temperatures and pollutants. The JPSS has a revisit of 4 days with a nadir spatial resolution of 50 km (field of regard) and swath width of 2800 km. Types of data products that can be derived from CrIS instrument data include carbon products (CO_2, CH_4, and CO).

The NASA-ISRO SAR mission (NISAR), launching in 2025, focuses on the cryosphere as a major area of interest. NISAR collects data in the *L*-band and the *S*-band, penetrating polar clouds and seasonal darkness. The NISAR swath of 240 km allows for a 12-day revisit and a 3–10 m resolution (mode dependent) [152]. With pointing control and a global orbit, NISAR will provide novel, year-round coverage of the Arctic surface and near-atmosphere. The mission will deliver complete, all-weather mapping of the ABZ freeze-thaw state, inundation, and soil moisture every 12 days [153]. Level 1 products provide the basis for subsidence applications as of interest for monitoring active layer dynamics. For AMPAC relevant Level-4 products are soil moisture and land inundation maps.

LandsatNext is expected to launch in late 2030. Compared to previous Landsat missions, the temporal and spatial resolution will be enhanced. Sensors will cover 26 bands. the spatial resolution will range from 10 to 60 m (TIR). The triplet constellation will allow for a repeat sampling interval of 6 days. This will be of benefit for monitoring wetlands and open water, specifically continuing the current generation of the European Sentinel-2 and complementing potentially Sentinel-2 next generation (not yet approved). Furthermore, this spatially-enhanced constellation will afford an opportunity to continue monitoring thermokarst development and surface signals and ecosystem response patterns to subsurface phenomena.

V. Parameter Specific Observation Requirements by GCOS

GCOS is defining requirements for a wide range of ECVs [154], [155]. Such specifications also drive future mission and service developments.

Relevant land observations are various soil properties including surface state, soil carbon, peatlands, land cover as proxy, and the state of permafrost expressed through ground temperature. Surface state and inundation are considered as ECVs but their requirements are defined considering the need for soil moisture product masking only. The target spatial resolution for soil moisture (1 km) is inadequate as it is too coarse to represent heterogeneous Arctic landscapes [52]. Requirements for permafrost ECVs (ground temperature and active layer thickness) have been so far only specified for in situ measurements [86]. Soil temperature is listed, but only down to a depth of 2 m. The active layer can extent further down [156] and seasonal temperature variations usually reach deeper [3].

Soil organic carbon is considered as an ECV down to a depth of 100 cm and at a spatial detail of 20–1000 km, which is

TABLE III
GCOS REQUIREMENTS FOR METHANE VARIABLES (SOURCE: [155])

	Requirements	Threshold	Breakthrough	Goal
CH_4 total column	Accuracy (2-sigma)	20 ppb	10 ppb	7 ppb
	Horizontal resolution	10 x 10 km2	1 x 1 km2	0.3 x 0.3 km2
	Observing cycle	3 days	subdaily (2/day)	1 h
CH_4 profile	Accuracy (2-sigma)	5 ppb	2 ppb	1 ppb
	Horizontal resolution	2000 x 2000 km	500 x 500 km	100 x 100 km2
	Vertical resolution	3 km	1 km	100 m
	Observing cycle	weekly (afternoon)	daily (afternoon)	hourly

insufficient for carbon-related applications in Arctic permafrost environments regarding spatial detail as well as depth. Peatland specifications better match the needs (20–1000 m) as well as high resolution land cover (goal $<$10 m).

GCOS requirements for methane concentrations are addressed for total column and profile measurements (see Table III). Overall, the target requirement of 300 $\times$ 300 m spatial resolution is coarse compared to the landscape changes. The upcoming hyperspectral missions meet the target requirement for the spatial resolution, while the hourly sampling, which would support diurnal emission analysis, is not achieved. The target profile requirements are spatially coarse (100 $\times$ 100 km) but vertically and temporally dense (100 m and hourly) and reflect more requirements for ground based observations. The GCOS terrestrial ECV parameter Anthropogenic CH_4 emissions is formulated by country and emission sector and is thus not relevant here (not included in Table III). Accuracy needs to be higher for monitoring of natural sources.

VI. DISCUSSION

Permafrost has never been the primary target of any satellite mission, although several missions focus on Arctic monitoring. However, relevant issues are addressed as part of secondary objectives in some approved missions. This includes several new Copernicus Expansion Missions (7 Sentinels) that have been identified by the European Commission (EC) as priorities for implementation in the coming years by providing new capabilities in support of current emerging user needs. This is complemented by two missions of the Scout program and one Earth Explorer mission (see Table I). The majority will focus on land surface remote sensing, except for the Copernicus Anthropogenic CO_2 Monitoring (CO2M) mission and the continuation of Sentinel-5P (precursor) with Sentinel-5, which both provide methane concentrations in the atmosphere. This will be complemented by the new ESA Scout mission (TANGO). Continuity is also targeted through the EUMETSAT/NOAA/NASA Joint Polar Satellite System (JPSS). Additional technical advance is expected from MERLIN (DLR and CNES).

The number of sensors available for the retrieval of XCH_4 will double by 2028 (see Fig. 1) and retrieval capabilities are expected to improve at the same time. These observations will be complemented by noncommercial missions which can identify point sources. But, the sensitivity will remain too low for natural sources as typical for Arctic environments. None of the upcoming satellite instruments will measure profiles. There is also a need for monitoring isotopes, which cannot be addressed with currently available technologies.

Rigorous validation is instrumental for the generation of upcoming satellite instruments. Concerning atmospheric CH4, FTS (TCCON/COCCON), balloons, aircore, and instruments on aircraft (remote sensing and in situ) are the backbone for validation activities. Ground-based measurements and flux tower measurements are needed but are insufficient, as they do not provide data products comparable to satellite observations. It is also possible to distinguish between 1) column measurements (in this case potentially different averaging kernels or weighting functions must be considered) using ground-based or airborne remote sensing; and 2) profile observations using balloon or aircraft. In the latter case, care has to be taken that the stratospheric part of the column is correctly accounted for. Further on, reference observations of profiles are needed for validating midtropospheric CH4 products of TIR instruments (e.g., IASI, IASI-NG).

More than 30 years of XCH_4 measurements will be available by 2032. The longest continuous record is available from AIRS on the Aqua platform with potentially 25 years. Maximum overlap of future and current missions is expected for 2029 (source: CEOS database, Fig. 2). This includes also non-European and NASA/NOAA missions. Combining historical data from SWIR and TIR sensors, e.g., IASI-NG and Sentinel-5p, with MWIR planned deployments of imaging spectrometers (e.g., NASA SBG) will provide the capability to resolve a more complete, spatiotemporal vertical profile of methane dispersion and transport across the Arctic. Japan and China are also upgrading their EO capabilities for GHG monitoring. Japanese (JAXA/NIES) GOSAT-GW (launch 2025) will continue GOSAT and GOSAT-2 GHG observations with added focus on the water cycle. It will carry two instruments, the imaging spectrometer measuring anthropogenic and natural CO_2 and CH_4 concentrations and the microwave radiometer to measure, e.g., precipitation, humidity, sea surface temperature, soil moisture, and snow water equivalent. Metop-SG, CO2M, Sentinel-5 and MERLIN are expected to be operating throughout this year together with Japan's GOSAT-GW and China's FY-3H (2024–). The Chinese TanSat follow-on mission, TanSat-2, will measure primarily CO_2 but also methane from medium-Earth elliptical orbit and large 1500 m swath covering latitudes up to 75 N with varying local times in 4x4 km nominal spatial resolution [157], similarly to FY-H3. TanSat-2 is planned for 2025–2027 what overlaps with FY-3H. Only CO2M is expected to be operational during the upcoming International Polar Year (IPY 2032/2033) according to current CEOS database records.

Satellite instruments typically rely on using relatively narrow spectral ranges for trace gas retrievals either in the SWIR or TIR for methane (or other spectral regions depending on the trace

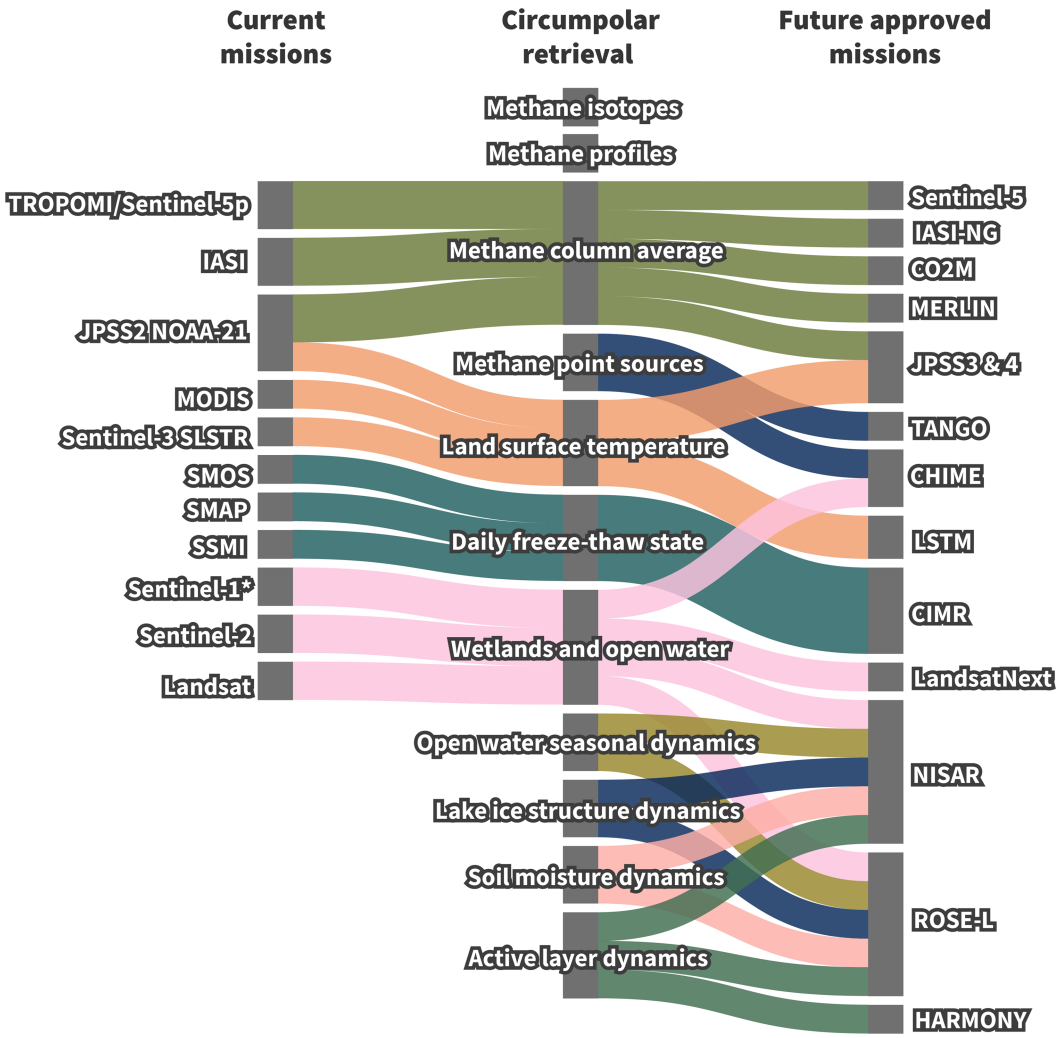

Fig. 1. NASA/NOAA and European current missions versus approved missions with AMPAC added value (see Table I) by parameter. ∗ Sentinel-1 also can provide information on active layer, surface state, open water, and soil moisture, but does not provide consistent data across the Arctic to quantify dynamics.

gas). Each spectral region is sensitive to a specific portion of the atmosphere, in the case of methane, SWIR is more sensitive to the surface, while TIR is sensitive to the midtroposphere [158]. Therefore, measurements using a specific spectral range leave a gap in the characterization of a portion of the atmosphere, for example, an SWIR instrument will not "see" methane transport in the free-troposphere (variations from transport are seen, transport model needed for usage), while a TIR instrument will not "see" methane sources at the surface.

This is problematic for understanding the methane dispersion and transport in the atmosphere. A step forward solving this problem is to perform multispectral retrievals by combining TIR and SWIR measurements, providing information from multiple layers of the atmosphere. In particular, this can be implemented using different instruments from multiple satellites and has been achieved in a number of cases. For example, multispectral multi-satellite retrievals at the spectral level (level 1) have been shown to improve sensitivity for methane and carbon monoxide [159], [160], as for lower tropospheric ozone [161], [162]. In addition to merging spectra from two individual sensors for a combined level 1 retrieval, synergistic level 2 combinations of satellite retrievals have also been shown to be effective in improving the sensitivity of methane retrievals, over and above retrievals from individual satellites [146].

Based on this heritage, there is the opportunity to combine TIR and SWIR information from current (e.g., IASI and Sentinel-5P) and future instruments such as IASI-NG and Sentinel-5 (on the same platform), to improve remote sensing of methane over challenging environments, such as the Arctic permafrost.

Smaller pixel sizes for retrieval of methane concentration will improve cloud-free observations, enabling scale-matching between satellite data, aircraft remote sensing, flux towers and in situ sampling. The MERLIN lidar will improve observation of the Arctic. In the long term, the quality of methane observations can benefit greatly from the synergistic use of lidar and passive remote sensing instruments, which need to be explored first on aircraft, and then on a common satellite platform.

There is also the potential for further research and development of existing algorithms in order to improve the coverage and data quality over the Arctic regions, for example by more

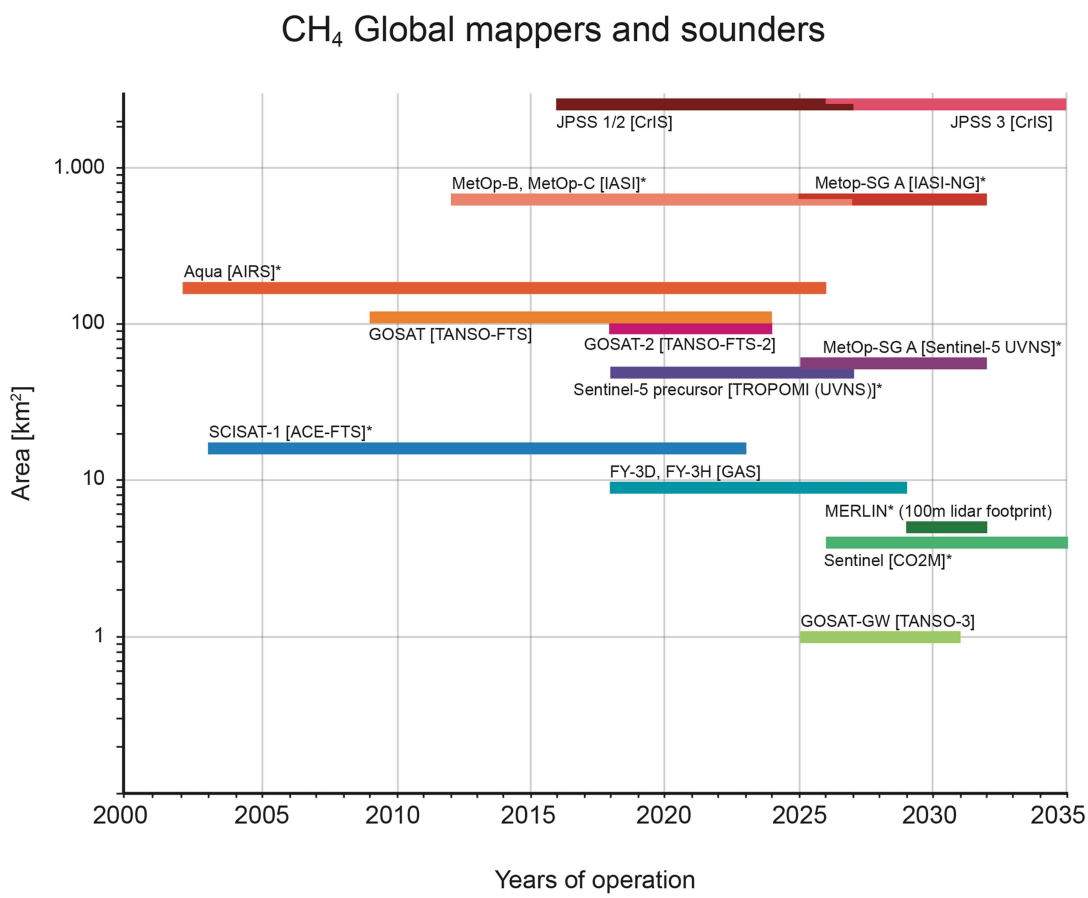

Fig. 2. Global mappers and sounders targeting retrieval of methane concentrations as included in the EOHandbook database (source: https://database.eohandbook.com/): Years of operation and area represented through nominal spatial resolution. ∗ indicates European, NASA/NOAA missions. Dashed line—current state. Colors are arbitrary and for differentiation only.

carefully chosen prior values or selective postfiltering. Hyperspectral and multispectral sensors might provide sufficient spatial detail and sensitivity to capture hotspots of natural methane emissions, but studies have been limited to airborne observations to date. In general, quantitative assessment of the potential improvements in spatial and temporal resolution, sensitivity, and accuracy would be beneficial for all sensor types.

Meteorological observations from satellites can provide valuable ancillary information, supporting 1) wind information which is crucial for the transport models that are required for inverse modeling; 2) knowledge about temperature, pressure and humidity profiles which is required for the retrieval of methane; 3) a better reanalysis of precipitation is also important for the general understanding of the hydrological cycle. The recently launched Arctic Weather Satellite [AWS—aka EPS-Sterna, a precursor for the multisatellite constellation EUMETSAT Polar System (EPS)], Aeolus-2 (planned for 2034, part of EPS, e.g., wind profiles), Atmosphere Observing System—Sky (planned for 2031, Canadian Space Agency) are thus also expected to provide advance for high latitude methane concentration retrieval.

Continuity of measurements is ensured for land variables, and the portfolio is widened through higher observation density. This will allow a step forward in observations of seasonal dynamics (see Fig. 1). The availability of passive microwave sensors from the considered space agencies will be reduced and limited to only one sensor (CIMR) considering approved missions. Multispectral medium resolution observations are continued and enhanced through LandsatNext from the NASA side. A Sentinel-2 follow-on would be crucial for advanced wetland and lake monitoring (higher repeat in combination with LandsatNext). Multiannual time series are currently only possible in some regions across the Arctic although availability of two satellites with the Sentinel-2 instrument [52]. In the near term, NASA's Plankton, Aerosol, Cloud, ocean Ecosystem (PACE, launched 8 February 2024) mission will also deliver spectral imaging of the pan-Arctic land surface but at 1 km spatial resolution [163]. NASA's Surface Biology and Geology (SBG) mission may also deliver pan-Arctic spectral imagery at 30 m spatial resolution [164] after 2028, with the potential to provide both detailed land surface classification and the potential detection of methane hotspots. But this mission is still in planning stage and currently defined land products foresee spatial detail similar to PACE. The Canadian mission WildFireSat (planned for 2028) is expected to complement land observations, although at comparably coarse spatial resolution (400 m (TIR, MWIR) and 200 m (NIR, VIS)).

The majority of land variables (wetlands, open water, soil moisture, surface deformation, and the state of the active layer)

require SAR acquisitions with consistent and frequent coverage. Although there have been many SAR missions in the past, the required coverage could not be achieved for Arctic ice-free land regions. This can be to a large extent attributed to prioritization issues. Arctic ice-free land areas are, in general, treated at the lowest priority level. The future *L*-band SAR missions NISAR and ROSE-L will therefore close a range of gaps if acquisition planning does consider the needs over high latitude permafrost regions. Such limitations, including temporal gaps, propagate as a result of short-term repeat-cycle mission planning. Combined use of *L*-band with *C*-band is expected to be of benefit for wetland monitoring (emerging vegetation detection). This requires "Companion" *C*-band SAR missions which acquire data at approximately the same time. Furthermore, novel SAR processing techniques, including change detection and hybrid ensemble learning frameworks, could help ameliorate the effects of these limitations and improve our understanding of how and to what extent Arctic change is occurring [165].

The accuracy of global surface soil moisture time series using microwaves is so far insufficient in Arctic regions [109], [110]. The foreseen soil moisture product from NISAR at 100 m resolution is therefore expected to allow for an advance in characterizing moisture gradients and dynamics, although the planned temporal (12 days) and spatial resolution are not expected to capture relevant processes in detail. National Research Council [166] specified a target resolution of 1 m for local studies, 100 m for circumpolar, and daily to weekly observations, respectively. The resolution of 100 m is not expected to capture typical gradients of Arctic tundra [52], [84]. CHIME can also be expected to provide added value for wetland-type mapping and their dynamics, but higher spatial resolution would also be needed in this case.

Crucial for land surface temperature observations is continuity and spatial detail. In general, the currently available spatial resolution is deemed insufficient for adequately modeling of ground temperature and active layer thickness, but used due to a lack of alternatives [86]. The combination with SAR, specifically InSAR, is expected to provide additional, spatially more detailed, information regarding active layer thaw state, but currently planned acquisition intervals for NISAR (12 days) may provide only limited insight into dynamics. Coarse resolution microwave sensors such as CIMR provide the necessary temporal sampling, but are limited to the upper surface only indicating the start of freeze-up or thaw. CIMR does, however, provide an advance due to a comparably high spatial resolution (5 km) for a passive microwave instrument and sub-daily acquisitions. With the two satellites, LSTM is expected to provide unprecedented detail. The high spatial detail obtained with thermal infrared observations (50 m) will allow for separation of the Arctic's typical small open water features from land area and heterogeneous land cover in general.

High-spatial-resolution thermal infrared land surface imaging will be revolutionized with the launch of the CNES-ISRO TRISHNA mission planned in 2026 [167], [168]. However, the coverage will be limited to maximum of 60 ° North, leaving out the vast majority of the permafrost region. LSTM and the planned NASA-ASI SBG-TIR mission [169] will also enable high accuracy mapping of evapotranspiration across the pan-Arctic to help balance Arctic hydrologic budgets and evaluate vegetation composition-function relationships. Working in coordination, this constellation promises daily or better land surface temperature (LST) maps. A prototype of the SBG-VSWIR mission hosted on the International Space Station (Earth Ventures Instrument EVI-4, since 2022) has been shown suitable for identification of geological methane sources [170], but is limited to areas south of 52°N.

The advance of new techniques such as GNSS remains to be clarified. Temporal sampling is limited. The added value through combined use with other microwave observations (SAR and passive) needs to be tested.

Altimeters such as the European CRISTAL mission will provide improved information on terrain change in general. However, the sensor is not sensitive enough for the comparably subtle changes associated with permafrost thaw [130]. The applicability will be limited to larger degradation features such as mega-slumps and water level change of larger water bodies. Integrating new lidar techniques, microsatellite constellations, and quantum-enhanced sensing—in parallel with altimeter and instrument advancements—could revolutionize detecting the subtle variability of permafrost degradation.

By the time of the International Polar Year 2032/2033, a wide range of European and US missions will be in operation, which will provide continuation or enhancement of land (CHIME, HARMONY, CRISTAL, ROSE-L, CIMR, LSTM, LandsatNext) as well as atmosphere (CO2M, MERLIN, JPSS, IASI-NG, and TANGO) observations relevant for AMPAC.

VII. Conclusion

By 2030, international Earth observations of the Arctic will be the most comprehensive since the beginning of the space program. A range of observational gaps are expected to be closed through enhanced availability of SAR, better spatial resolution for retrievals of column methane concentrations, and hotspot identification. The latter will be, however, of limited use for the Arctic permafrost region due to the fact that natural wetland CH_4 emissions are orders of magnitude lower than man-made emission point sources. The currently approved missions will nevertheless provide a basis to tackle the AMPAC goals, specifically through the exploitation of the increasing Earth observation capacity.

Airborne hyperspectral studies have demonstrated the applicability of imaging spectroscopy for natural sources of methane in permafrost regions. However, space based-studies are still lacking due to a lack of suitable operational hyperspectral satellite sensors until now. Higher spatial detail for land cover observations than available to date will not be achieved, but an advance in monitoring temporal dynamics (specifically through new SAR missions) and thematic content through improved spectral capabilities will be enabled. A step forward is expected for complementary observations such as for land surface temperature from new higher resolution thermal infrared sensors and lake ice structure from new SAR missions. Relevant analyses need to be fostered in order to support the AMPAC goals.

TABLE IV
ORBIT CHARACTERISTICS INCLUDING ORBIT ALTITUDE, INCLINATION, AND LOCAL TIME OF ASCENDING NODE (LTAN) OF THE ATMOSPHERIC METHANE SENSORS (SEE TABLE I AND FIGS. 1 AND 2) (SOURCE: HTTPS://DATABASE.EOHANDBOOK.COM/)

Mission	Instrument	Period	Orbit altitude [km]	Inclination [°]	LTAN
ENVISAT	SCIAMACHY	2001–2012	782	98.5	10:30
GOSAT	TANSO-FTS	2009 –	666	98	13:00
Sentinel-5P	TROPOMI	2017 –	824	98.7	13.30
METOP	IASI	2006 –)[1]	817	98.7	09:30
Suomi NPP	CrIS	2011 –	824	98.7	13:30
JPSS	CrIS	2017 –)[2]	833	98.8	13:30
GOSAT-2	TANSO-FTS-2	2018 –	613	97.8	13:00
GOSAT-2	TANSO-FTS-2	2018 –	613	97.8	13:00
METOP-SG	IASI-NG	2025 –)[3]	824	98.7	09:30
GOSAT-GW	TANSO-3	2025 –	666	98.1	13:30
Sentinel-5	UVNS	2025 –)[4]	824	98.0	09:30
CO2M	CO2I	2026 –	735	97.7	11:30
MERLIN	IPDA lidar	2029 –	500	97.4	06:00 or 18:00 (tbd)

[1] METOP-A: 2006-2021; METOP-B: 2012-2024; METOP-C: 2018-2027
[2] JPSS-1 (NOAA-20): 2017-2027; JPSS-2: 2022-2028; JPSS-3: 2026-2035. Planned: JPSS-4: 2031-2038,
[3] METOP-SG A1: 2025-2032; planned: METOP-SG A2: 2032-2039; METOP-SG A3: 2039-2046
[4] The Sentinel-5 payload instrument is hosted as a customer furnished item on the METOP-SG a satellites.

Monitoring the state of permafrost requires a paradigm shift in how we design and deploy satellite missions. Active remote sensing of atmospheric CH_4 will increase our understanding of cold season emissions. In general, all approved future satellite missions targeting concentrations are expected to improve seasonal and diurnal observations. New missions to be launched in the next years (2025–2026) will provide higher spatial detail than previously available from the noncommercial sector. This development alone will allow a step forward, but key will be missions further ahead.

Data continuity with back-to-back satellite missions providing openly available data is important in order to capture trends and rates of change in the rapidly changing Arctic. High spatial and temporal resolution is essential for all relevant parameters in order to bridge the gap between T-D and B-U estimates of methane fluxes across northern hemisphere permafrost regions. Airborne observations remain important for scaling and validation, in addition to actual field data.

A broad portfolio of hyperspectral, passive microwave, synthetic aperture radar, altimeter, land surface temperature, and lidar measurements in addition to imaging spectrometers will be available by 2032/2033, at the time of the International Polar Year, for tasks useful for reaching many AMPAC goals. This sensor suite will allow for comprehensive advanced experiments and a focus during IPY should be the implementation of suitable in situ observation campaigns to maximize synergies, facilitate validation across different terrain and permafrost ecosystems, and allow data-driven scaling efforts for Arctic methane dynamics. Around 2029, maximum overlap is expected for sensors targeting methane concentration retrieval which poses an opportunity for benchmarking. The new missions are expected to substantially advance our understanding of methane dynamics from permafrost regions.

APPENDIX

See Tables IV and V.

ACKNOWLEDGMENT

This work evolved from the NASA-ESA Arctic Methane and Permafrost Challenge (AMPAC).

TABLE V
ORBIT CHARACTERISTICS INCLUDING ORBIT ALTITUDE, INCLINATION, AND LOCAL TIME OF ASCENDING NODE (LTAN) OF THE HYPERSPECTRAL IMAGERS (SEE TABLE I AND FIGS. 1 AND 2)

Mission	Instrument	Period	Orbit [km]	Inclination [°]	LTAN
PRISMA	HYC	2019–	615	97.9	10:30
ENMAP	HSI	2022–	650	98.0	11:00
CHIME	HSI	2020–	632	97.9	10:45

REFERENCES

[1] IPCC, *IPCC Special Report on the Ocean and Cryosphere in a Changing Climate*, H.-O. Pörtner et al. Eds. Cambridge Univ. Press, 2019.
[2] M. Rantanen et al., "The arctic has warmed nearly four times faster than the globe since 1979," *Commun. Earth Environ.*, vol. 3, Aug. 2022, Art. no. 168.
[3] B. K. Biskaborn et al., "Permafrost is warming at a global scale," *Nature Commun.*, vol. 10, Jan. 2019, Art. no. 264 .
[4] S. L. Smith, H. B. O'Neill, K. Isaksen, J. Noetzli, and V. E. Romanovsky, "The changing thermal state of permafrost," *Nature Rev. Earth Environ.*, vol. 3, pp. 10–23, Jan. 2022.
[5] M. R. England, I. Eisenman, N. J. Lutsko, and T. J. W. Wagner, "The recent emergence of Arctic amplification," *Geophysical Res. Lett.*, vol. 48, Aug. 2021, Art. no. e2021GL094086.
[6] M. Previdi, K. L. Smith, and L. M. Polvani, "Arctic amplification of climate change: A review of underlying mechanisms," *Environ. Res. Lett.*, vol. 16, Sep. 2021, Art. no. 093003.
[7] E. A. Schuur et al., "Permafrost and climate change: Carbon cycle feedbacks from the warming arctic," *Annu. Rev. Environ. Resour.*, vol. 47, pp. 343–371, Oct. 2022.
[8] G. Hugelius et al., "Estimated stocks of circumpolar permafrost carbon with quantified uncertainty ranges and identified data gaps," *Biogeosciences*, vol. 11, no. 23, pp. 6573–6593, 2014.
[9] G. Grosse, V. Romanovsky, T. Jorgenson, K. W. Anthony, J. Brown, and P. P. Overduin, "Vulnerability and feedbacks of permafrost to climate change," *Eos, Trans. Amer. Geophysical Union*, vol. 92, pp. 73–74, Mar. 2011.
[10] K. Walter Anthony et al., "21st-century modeled permafrost carbon emissions accelerated by abrupt thaw beneath lakes," *Nature Commun.*, vol. 9, Aug. 2018, Art. no. 3262.
[11] M. R. Turetsky et al., "Carbon release through abrupt permafrost thaw," *Nature Geosci.*, vol. 13, pp. 138–143, Feb. 2020.
[12] S. Wittig et al., "Estimating methane emissions in the arctic nations using surface observations from 2008 to 2019," *Atmospheric Chem. Phys.*, vol. 23, pp. 6457–6485, Jun. 2023.
[13] M. Saunois et al., "Global methane budget 2000–2020," *Earth Syst. Sci. Data Discuss.* [accepted preprint], Jun. 2024, doi: 10.5194/essd-2024-115.

[14] F.-J. W. Parmentier et al., "A synthesis of the arctic terrestrial and marine carbon cycles under pressure from a dwindling cryosphere," *Ambio*, vol. 46, pp. 53–69, Jan. 2017.

[15] N. Rößger, T. Sachs, C. Wille, J. Boike, and L. Kutzbach, "Seasonal increase of methane emissions linked to warming in Siberian tundra," *Nature Climate Change*, vol. 12, pp. 1031–1036, Oct. 2022.

[16] G. Hugelius et al., "Two decades of permafrost region CO_2, CH_4, and N_2O budgets suggest a small net greenhouse gas source to the atmosphere," Sep. 2023.

[17] M. Saunois et al., "The global methane budget 2000–2017," *Earth Syst. Sci. Data*, vol. 12, pp. 1561–1623, Jul. 2020.

[18] L. C. Smith, Y. Sheng, and G. M. MacDonald, "A first pan-arctic assessment of the influence of glaciation, permafrost, topography and peatlands on northern hemisphere lake distribution," *Permafrost Periglacial Processes*, vol. 18, pp. 201–208, Apr. 2007.

[19] L. Brosius et al., "Spatiotemporal patterns of northern lake formation since the last glacial maximum," *Quaternary Sci. Rev.*, vol. 253, Feb. 2021, Art. no. 106773.

[20] P. A. Keddy et al., "Wet and wonderful: The world's largest wetlands are conservation priorities," *BioScience*, vol. 59, pp. 39–51, Jan. 2009.

[21] G. Grosse, B. Jones, and C. Arp, *8.21 Thermokarst Lakes, Drainage, and Drained Basins*. Amsterdam, Netherlands: Elsevier, 2013, pp. 325–353.

[22] B. M. Jones et al., "Lake and drained lake basin systems in lowland permafrost regions," *Nature Rev. Earth Environ.*, vol. 3, pp. 85–98, Jan. 2022.

[23] D. Olefeldt et al., "The Boreal–Arctic wetland and lake dataset (BAWLD)," *Earth Syst. Sci. Data*, vol. 13, pp. 5127–5149, Nov. 2021.

[24] J. Ramage et al., "The net GHG balance and budget of the permafrost region (2000–2020) from ecosystem flux upscaling," *Glob. Biogeochemical Cycles*, vol. 38, Apr. 2024, Art. no. e2023GB007953.

[25] D. Zona et al., "Cold season emissions dominate the Arctic tundra methane budget," *Proc. Nat. Acad. Sci.*, vol. 113, pp. 40–45, Dec. 2015.

[26] C. C. Treat, A. A. Bloom, and M. E. Marushchak, "Nongrowing season methane emissions–a significant component of annual emissions across northern ecosystems," *Glob. Change Biol.*, vol. 24, pp. 3331–3343, Apr. 2018.

[27] L. Bruhwiler, F.-J. W. Parmentier, P. Crill, M. Leonard, and P. I. Palmer, "The arctic carbon cycle and its response to changing climate," *Curr. Climate Change Rep.*, vol. 7, pp. 14–34, Feb. 2021.

[28] T. Bao, X. Xu, G. Jia, D. P. Billesbach, and R. C. Sullivan, "Much stronger tundra methane emissions during autumn freeze than spring thaw," *Glob. Change Biol.*, vol. 27, pp. 376–387, Nov. 2020.

[29] J. A. Rosentreter et al., "Revisiting the global methane cycle through expert opinion," *Earth's Future*, vol. 12, Jun. 2024, Art. no. e2023EF004234.

[30] J. L. McCarty et al., "Reviews and syntheses: Arctic fire regimes and emissions in the 21st century," *Biogeosciences*, vol. 18, pp. 5053–5083, Sep. 2021.

[31] V.-V. Paunu, J. L. McCarty, A. Lipsanen, and I. Entsalo1, "Fire in the Arctic: Current trends and future pathways. Arctic black carbon impacting on climate and air pollution (ABC-iCAP) project technical report," SYKE, NASA, Tech. Rep. 1, Nov. 2023, p. 20.

[32] C. M. Gibson, L. E. Chasmer, D. K. Thompson, W. L. Quinton, M. D. Flannigan, and D. Olefeldt, "Wildfire as a major driver of recent permafrost thaw in Boreal peatlands," *Nature Commun.*, vol. 9, Aug. 2018, Art. no. 3041.

[33] X.-Y. Li et al., "Influences of forest fires on the permafrost environment: A review," *Adv. Climate Change Res.*, vol. 12, pp. 48–65, Feb. 2021.

[34] C. A. Phillips et al., "Escalating carbon emissions from North American boreal forest wildfires and the climate mitigation potential of fire management," *Sci. Adv.*, vol. 8, Apr. 2022, Art. no. eabl7161.

[35] B. M. Jones et al., "Recent arctic tundra fire initiates widespread thermokarst development," *Sci. Rep.*, vol. 5, Oct. 2015, Art. no. 15865.

[36] M. Morgunova, "Why is exploitation of arctic offshore oil and natural gas resources ongoing? A multi-level perspective on the cases of Norway and Russia," *Polar J.*, vol. 10, pp. 64–81, Jan. 2020.

[37] A. Tsuruta et al., "CH_4 fluxes derived from assimilation of Tropomi XCH_4 in carbontracker Europe-CH_4: Evaluation of seasonality and spatial distribution in the northern high latitudes," *Remote Sens.*, vol. 15, Mar. 2023, Art. no. 1620.

[38] S. M. Natali et al., "Permafrost carbon feedbacks threaten global climate goals," *Proc. Nat. Acad. Sci.*, vol. 118, May 2021, Art. no. e2100163118.

[39] C. Sweeney et al., "No significant increase in long-term CH_4 emissions on north slope of Alaska despite significant increase in air temperature," *Geophysical Res. Lett.*, vol. 43, pp. 6604–6611, Jun. 2016.

[40] K. R. Miner et al., "Permafrost carbon emissions in a changing arctic," *Nature Rev. Earth Environ.*, vol. 3, pp. 55–67, Jan. 2022.

[41] N. J. Pastick, M. T. Jorgenson, B. K. Wylie, S. J. Nield, K. D. Johnson, and A. O. Finley, "Distribution of near-surface permafrost in Alaska: Estimates of present and future conditions," *Remote Sens. Environ.*, vol. 168, pp. 301–315, Oct. 2015.

[42] W. Steffen et al., "Trajectories of the earth system in the anthropocene," *Proc. Nat. Acad. Sci.*, vol. 115, pp. 8252–8259, Aug. 2018.

[43] E. A. G. Schuur et al., "Climate change and the permafrost carbon feedback," *Nature*, vol. 520, pp. 171–179, Apr. 2015.

[44] C. D. Koven, D. M. Lawrence, and W. J. Riley, "Permafrost carbon-climate feedback is sensitive to deep soil carbon decomposability but not deep soil nitrogen dynamics," *Proc. Nat. Acad. Sci.*, vol. 112, pp. 3752–3757, Mar. 2015.

[45] E. J. Burke et al., "Quantifying uncertainties of permafrost carbon-climate feedbacks," *Biogeosciences*, vol. 14, pp. 3051–3066, Jun. 2017.

[46] D. M. Lawrence, C. D. Koven, S. C. Swenson, W. J. Riley, and A. G. Slater, "Permafrost thaw and resulting soil moisture changes regulate projected high-latitude CO_2 and CH_4 emissions," *Environ. Res. Lett.*, vol. 10, Sep. 2015, Art. no. 094011.

[47] L. M. Farquharson, V. E. Romanovsky, A. Kholodov, and D. Nicolsky, "Sub-aerial Talik formation observed across the discontinuous permafrost zone of Alaska," *Nature Geosci.*, vol. 15, pp. 475–481, Jun. 2022.

[48] K. M. Walter Anthony et al., "Upland Yedoma Taliks are an unpredicted source of atmospheric methane," *Nature Commun.*, vol. 15, Jul. 2024, Art. no. 6056.

[49] C. C. Treat et al., "Permafrost carbon: Progress on understanding stocks and fluxes across northern terrestrial ecosystems," *J. Geophysical Res.: Biogeosciences*, vol. 129, Feb. 2024, Art. no. e2023JG007638.

[50] M. M. T. A. Pallandt et al., "Representativeness assessment of the pan-arctic eddy covariance site network and optimized future enhancements," *Biogeosciences*, vol. 19, pp. 559–583, Feb. 2022.

[51] J. Schneider, G. Grosse, and D. Wagner, "Land cover classification of tundra environments in the Arctic Lena Delta based on Landsat 7 ETM data and its application for upscaling of methane emissions," *Remote Sens. Environ.*, vol. 113, 2009, Art. no. 380.

[52] A. Bartsch et al., "Circumarctic land cover diversity considering wetness gradients," *Hydrol. Earth Syst. Sci.*, vol. 28, pp. 2421–2481, Jun. 2024.

[53] M. Engram et al., "Remote sensing northern lake methane ebullition," *Nature Climate Change*, vol. 10, pp. 511–517, May 2020.

[54] G. Pointner and A. Bartsch, "Mapping arctic lake ice backscatter anomalies using Sentinel-1 time series on Google Earth engine," *Remote Sens.*, vol. 13, Apr. 2021, Art. no. 1626.

[55] K. Böttcher et al., "Proxy indicators for mapping the end of the vegetation active period in boreal forests inferred from satellite-observed soil freeze and era-interim reanalysis air temperature," *J. Photogrammetry, Remote Sens. Geoinf. Sci.*, vol. 86, pp. 169–185, Oct. 2018.

[56] D. J. Jacob et al., "Quantifying methane emissions from the global scale down to point sources using satellite observations of atmospheric methane," *Atmospheric Chem. Phys.*, vol. 22, pp. 9617–9646, Jul. 2022.

[57] C. D. Elder et al., "Characterizing methane emission hotspots from thawing permafrost," *Glob. Biogeochemical Cycles*, vol. 35, Dec. 2021, Art. no. e2020GB006922.

[58] D. J. Varon, D. Jervis, J. McKeever, I. Spence, D. Gains, and D. J. Jacob, "High-frequency monitoring of anomalous methane point sources with multispectral Sentinel-2 satellite observations," *Atmos. Meas. Techn.*, vol. 14, pp. 2771–2785, Apr. 2021.

[59] G. Ehret et al., "Merlin: A french-german space LiDAR mission dedicated to atmospheric methane," *Remote Sens.*, vol. 9, Oct. 2017, Art. no. 1052.

[60] R. O. Green et al., "The earth surface mineral dust source investigation: An earth science imaging spectroscopy mission," in *Proc. 2020 IEEE Aerosp. Conf.*, 2020, pp. 1–15.

[61] M. Gottwald et al., "Nine years of atmospheric remote sensing with SCIAMACHY - instrument performance," in *Proc. IEEE Int. Geosci. Remote Sens. Symp.*, Jul. 2011, pp. 3538–3541.

[62] A. Kuze, H. Suto, M. Nakajima, and T. Hamazaki, "Thermal and near infrared sensor for carbon observation Fourier-transform spectrometer on the greenhouse gases observing satellite for greenhouse gases monitoring," *Appl. Opt.*, vol. 48, pp. 6716–6733, Dec. 2009.

[63] R. Imasu et al., "Greenhouse gases observing SATellite 2 (GOSAT-2): Mission overview," *Prog. Earth Planet. Sci.*, vol. 10, pp. 1–35, Dec. 2023.

[64] A. de Lange and J. Landgraf, "Methane profiles from GOSAT thermal infrared spectra," *Atmos. Meas. Techn.*, vol. 11, pp. 3815–3828, Jun. 2018.

[65] H. Lindqvist et al., "Evaluation of sentinel-5p Tropomi methane observations at northern high latitudes," *Remote Sens.*, vol. 16, Aug. 2024, Art. no. 2979.

[66] E. Dowd et al., "First validation of high-resolution satellite-derived methane emissions from an active gas leak in the U.K.," *Atmos. Meas. Techn.*, vol. 17, pp. 1599–1615, Mar. 2024.

[67] B. J. Schuit et al., "Automated detection and monitoring of methane super-emitters using satellite data," *Atmos. Chem. Phys.*, vol. 23, pp. 9071–9098, Sep. 2023.

[68] R. Siddans et al., "Global height-resolved methane retrievals from the infrared atmospheric sounding interferometer (IASI) on metop," *Atmos. Meas. Techn.*, vol. 10, pp. 4135–4164, Nov. 2017.

[69] S. Massart et al., "Assimilation of atmospheric methane products into the Macc-II system: From Sciamachy to Tanso and Iasi," *Atmos. Chem. Phys.*, vol. 14, pp. 6139–6158, Jun. 2014.

[70] L. Yurganov, F. Muller-Karger, and I. Leifer, "Enhanced methane emission from arctic seas in winter: Satellite data," in *New Prospects in Environmental Geosciences and Hydrogeosciences*, H. Chenchouni, Eds. Cham, Switzerland: Springer, 2022, pp. 41–44.

[71] E. Jurado et al., "IASI-NG system: An overview of the current design and performances," in *Proc. IEEE Int. Geosci. Remote Sens. Symp.*, 2022, pp. 6471–6474.

[72] N. Smith and C. D. Barnet, "CLIMCAPS observing capability for temperature, moisture, and trace gases from AIRS/AMSU and CrIS/ATMS," *Atmos. Meas. Techn.*, vol. 13, pp. 4437–4459, 2020.

[73] Y. Han et al., "Suomi NPP CrIS measurements, sensor data record algorithm, calibration and validation activities, and record data quality," *J. Geophysical Res.: Atmos.*, vol. 118, pp. 12,734–12,748, Nov. 2013.

[74] G. Ehret, C. Kiemle, M. Wirth, A. Amediek, A. Fix, and S. Houweling, "Space-borne remote sensing of CO_2, CH_4, and N_2O by integrated path differential absorption LiDAR: A sensitivity analysis," *Appl. Phys. B*, vol. 90, pp. 593–608, Jan. 2008.

[75] S. Kawa et al., "Active sensing of CO_2 emissions over nights, days, and seasons (ASCENDS): Final report of the ascends ad hoc science definition team," Tech. Rep. NASA/TP-2018-219034, 11 2018.

[76] J. Caron, Y. Durand, J.-L. Bezy, and R. Meynart, "Performance modeling for a-scope: A space-borne LiDAR measuring atmospheric CO_2," *Proc. SPIE*, vol. 7479, Sep. 2009, Art. no. 74790E.

[77] C. Fan et al., "Preliminary analysis of global column-averaged CO_2 concentration data from the spaceborne aerosol and carbon dioxide detection Lidar onboard AEMS," *Opt. Exp.*, vol. 32, May 2024, Art. no. 21870.

[78] W. Chen et al., *Spaceborne Aerosol and Carbon Dioxide Detection Lidar (ACDL) Status and Progress*. Berlin, Germany: Springer, 2024, pp. 97–107.

[79] A. K. Thorpe, D. A. Roberts, E. S. Bradley, C. C. Funk, P. E. Dennison, and I. Leifer, "High resolution mapping of methane emissions from marine and terrestrial sources using a cluster-tuned matched filter technique and imaging spectrometry," *Remote Sens. Environ.*, vol. 134, pp. 305–318, Jul. 2013.

[80] R. F. Kokaly et al., "USGS spectral library version 7: U.S. Geological Survey Data Series 1035", p. 61, 2017, doi: 10.3133/ds1035.

[81] C. D. Elder, D. R. Thompson, A. K. Thorpe, P. Hanke, K. M. Walter Anthony, and C. E. Miller, "Airborne mapping reveals emergent power law of arctic methane emissions," *Geophysical Res. Lett.*, vol. 47, Feb. 2020, Art. no. e2019GL085707.

[82] L. K. Clayton et al., "Active layer thickness as a function of soil water content," *Environ. Res. Lett.*, vol. 16, May 2021, Art. no. 055028.

[83] J. Palmtag et al., "A high spatial resolution soil carbon and nitrogen dataset for the northern permafrost region based on circumpolar land cover upscaling," *Earth Syst. Sci. Data*, vol. 14, pp. 4095–4110, Sep. 2022.

[84] M. B. Siewert, J. Hanisch, N. Weiss, P. Kuhry, T. C. Maximov, and G. Hugelius, "Comparing carbon storage of Siberian tundra and Taiga permafrost ecosystems at very high spatial resolution," *J. Geophysical Res.: Biogeosciences*, vol. 120, no. 10, pp. 1973–1944, 2015.

[85] A. Bartsch, A. Höfler, C. Kroisleitner, and A. M. Trofaier, "Land cover mapping in northern high latitude permafrost regions with satellite data: Achievements and remaining challenges," *Remote Sens.*, vol. 8, no. 12, 2016, Art. no. 979.

[86] A. Bartsch, T. Strozzi, and I. Nitze, "Permafrost monitoring from space," *Surv. Geophys.*, vol. 44, pp. 1579–1613, Mar. 2023.

[87] M. K. Raynolds et al., "A raster version of the circumpolar arctic vegetation map (CAVM)," *Raynolds*, vol. 232, 2019, Art. no. 111297.

[88] B. Widhalm, A. Bartsch, and B. Heim, "A novel approach for the characterization of tundra wetland regions with C-band SAR satellite data," *Int. J. Remote Sens.*, vol. 36, no. 22, pp. 5537–5556, 2015.

[89] S. Lisovski et al., "A new habitat map of the Lena delta in Arctic Siberia based on field and remote sensing datasets," Feb. 2023.

[90] T. Virtanen and M. Ek, "The fragmented nature of Tundra landscape," *Int. J. Appl. Earth Observ. Geoinf.*, vol. 27, pp. 4–12, Apr. 2014.

[91] M. J. Lara et al., "Polygonal tundra geomorphological change in response to warming alters future Co_2 and CH_4 flux on the barrow peninsula," *Glob. Change Biol.*, vol. 21, pp. 1634–1651, Nov. 2014.

[92] G. Hugelius et al., "High-resolution mapping of ecosystem carbon storage and potential effects of permafrost thaw in periglacial terrain, European Russian arctic," *J. Geophysical Res.*, vol. 116, 2011, Art. no. G03024.

[93] S. Sjögersten et al., "Optical and radar earth observation data for upscaling methane emissions linked to permafrost degradation in sub-arctic peatlands in northern Sweden," *Biogeosciences*, vol. 20, pp. 4221–4239, Oct. 2023.

[94] M. Wik, R. K. Varner, K. W. Anthony, S. MacIntyre, and D. Bastviken, "Climate-sensitive northern lakes and ponds are critical components of methane release," *Nature Geosci.*, vol. 9, pp. 99–105, Jan. 2016.

[95] E. E. Webb, A. K. Liljedahl, J. A. Cordeiro, M. M. Loranty, C. Witharana, and J. W. Lichstein, "Permafrost thaw drives surface water decline across lake-rich regions of the arctic," *Nature Climate Change*, vol. 12, pp. 841–846, Aug. 2022.

[96] I. Nitze et al., "Landsat-based trend analysis of lake dynamics across northern permafrost regions," *Remote Sens.*, vol. 9, Jun. 2017, Art. no. 640.

[97] M. J. Lara, Y. Chen, and B. M. Jones, "Recent warming reverses forty-year decline in catastrophic lake drainage and hastens gradual lake drainage across Northern Alaska," *Environ. Res. Lett.*, vol. 16, Nov. 2021, Art. no. 124019.

[98] E. Matthews, M. S. Johnson, V. Genovese, J. Du, and D. Bastviken, "Methane emission from high latitude lakes: Methane-centric lake classification and satellite-driven annual cycle of emissions," *Sci. Rep.*, vol. 10, Jul. 2020, Art. no. 12465.

[99] A. Bartsch et al., "Seasonal progression of ground displacement identified with satellite radar interferometry and the impact of unusually warm conditions on permafrost at the Yamal peninsula in 2016," *Remote Sens.*, vol. 11, Aug. 2019, Art. no. 1865.

[100] H. Bergstedt et al., "Deriving a frozen area fraction from metop ASCAT backscatter based on Sentinel-1," *IEEE Trans. Geosci. Remote Sens.*, vol. 58, pp. 6008–6019, Sep. 2020.

[101] I. Nitze, G. Grosse, B. M. Jones, V. E. Romanovsky, and J. Boike, "Remote sensing quantifies widespread abundance of permafrost region disturbances across the arctic and subarctic," *Nature Commun.*, vol. 9, Dec. 2018, Art. no. 5423 .

[102] A. Runge, I. Nitze, and G. Grosse, "Remote sensing annual dynamics of rapid permafrost thaw disturbances with LandTrendr," *Remote Sens. Environ.*, vol. 268, Jan. 2022, Art. no. 112752.

[103] C. Knoblauch et al., "Carbon dioxide and methane release following abrupt thaw of pleistocene permafrost deposits in Arctic Siberia," *J. Geophysical Res.: Biogeosciences*, vol. 126, Nov. 2021, Art. no. e2021JG006543.

[104] J. Heslop et al., "A synthesis of methane dynamics in thermokarst lake environments," *Earth Sci. Rev.*, vol. 210, Nov. 2020, Art. no. 103365.

[105] M. J. Lara et al., "Local-scale arctic tundra heterogeneity affects regional-scale carbon dynamics," *Nature Commun.*, vol. 11, Oct. 2020, Art. no. 4925.

[106] J. Reschke, A. Bartsch, S. Schlaffer, and D. Schepaschenko, "Capability of C-band SAR for operational wetland monitoring at high latitudes," *Remote Sens.*, vol. 4, pp. 2923–2943, 2012.

[107] A. Bartsch, B. Widhalm, P. Kuhry, G. Hugelius, J. Palmtag, and M. Siewert, "Can c-band SAR be used to estimate soil organic carbon storage in tundra?," *Biogeosciences*, vol. 13, pp. 5453–5470, 2016.

[108] J. D. Watts, J. S. Kimball, A. Bartsch, and K. C. McDonald, "Surface water inundation in the Boreal-Arctic: Potential impacts on regional methane emissions," *Environ. Res. Lett.*, vol. 9, Jun. 2014, Art. no. 075001.

[109] E. Wrona, T. L. Rowlandson, M. Nambiar, A. A. Berg, A. Colliander, and P. Marsh, "Validation of the soil moisture active passive (SMAP) satellite soil moisture retrieval in an arctic Tundra environment," *Geophysical Res. Lett.*, vol. 44, pp. 4152–4158, May 2017.

[110] E. Högström, B. Heim, A. Bartsch, H. Bergstedt, and G. Pointner, "Evaluation of a MetOp ASCAT-derived surface soil moisture product in Tundra environments," *J. Geophysical Res.: Earth Surf.*, vol. 123, pp. 3190–3205, Dec. 2018.

[111] J. Ortet et al., "Evaluating soil moisture retrieval in arctic and sub-Arctic environments using passive microwave satellite data," *Int. J. Digit. Earth*, vol. 17, Aug. 2024, Art. no. 2385079.

[112] Y. A. Y. Albuhaisi, Y. van der Velde, R. De Jeu, Z. Zhang, and S. Houweling, "High-resolution estimation of methane emissions from boreal and pan-arctic wetlands using advanced satellite data," *Remote Sens.*, vol. 15, Jul. 2023, Art. no. 3433.

[113] R. Zhang, S. Chan, R. Bindlish, and V. Lakshmi, "A performance analysis of soil dielectric models over organic soils in Alaska for passive microwave remote sensing of soil moisture," *Remote Sens.*, vol. 15, Mar. 2023, Art. no. 1658.

[114] L. Liu, T. Zhang, and J. Wahr, "InSAR measurements of surface deformation over permafrost on the north slope of Alaska," *J. Geophysical Res.: Earth Surf.*, vol. 115, Aug. 2010, Art. no. F03023.

[115] T. Strozzi et al., "Sentinel-1 SAR interferometry for surface deformation monitoring in low-land permafrost areas," *Remote Sens.*, vol. 10, Aug. 2018, Art. no. 1360.

[116] J. Obu et al., "ESA permafrost climate change initiative (Permafrost_CCI): Permafrost ground temperature for the northern hemisphere, v3.0," CEDA, 2021. Accessed: Feb. 14, 2025. [Online]. Available: http://catalogue.ceda.ac.uk/uuid/8239d5f6263f4551bf2bd100d3ecbead/

[117] S. Westermann et al., "Transient modeling of the ground thermal conditions using satellite data in the Lena river delta, Siberia," *Cryosphere*, vol. 11, pp. 1441–1463, Jun. 2017.

[118] C. Derksen et al., "Retrieving landscape freeze/thaw state from soil moisture active passive (SMAP) radar and radiometer measurements," *Remote Sens. Environ.*, vol. 194, pp. 48–62, Jun. 2017.

[119] K. Rautiainen et al., "Smos prototype algorithm for detecting autumn soil freezing," *Remote Sens. Environ.*, vol. 180, pp. 346–360, Jul. 2016.

[120] Y. Kim, J. S. Kimball, J. Glassy, and J. Du, "An extended global earth system data record on daily landscape freeze–thaw status determined from satellite passive microwave remote sensing," *Earth System Sci. Data*, vol. 9, pp. 133–147, Feb. 2017.

[121] V. Naeimi et al., "ASCAT surface state flag (SSF): Extracting information on surface freeze/thaw conditions from backscatter data using an empirical threshold-analysis algorithm," *IEEE Trans. Geosci. Remote Sens.*, vol. 50, pp. 2566–2582, Jul. 2012.

[122] C. Kroisleitner, A. Bartsch, and H. Bergstedt, "Circumpolar patterns of potential mean annual ground temperature based on surface state obtained from microwave satellite data," *Cryosphere*, vol. 12, pp. 2349–2370, Jul. 2018.

[123] J. Cohen et al., "A modeling-based approach for soil frost detection in the northern boreal forest region with C-band SAR," *IEEE Trans. Geosci. Remote Sens.*, vol. 57, pp. 1069–1083, Feb. 2019.

[124] J. Cohen, K. Rautiainen, J. Lemmetyinen, T. Smolander, J. Vehviläinen, and J. Pulliainen, "Sentinel-1 based soil freeze/thaw estimation in boreal forest environments," *Remote Sens. Environ.*, vol. 254, Mar. 2021, Art. no. 112267.

[125] H. Bergstedt and A. Bartsch, "Surface state across scales; temporal and spatial patterns in land surface freeze/thaw dynamics," *Geosciences*, vol. 7, 2017, Art. no. 65.

[126] H. Bergstedt, S. Zwieback, A. Bartsch, and M. Leibman, "Dependence of C-band backscatter on ground temperature, air temperature and snow depth in Arctic permafrost regions," *Remote Sens.*, vol. 10, Jan. 2018, Art. no. 142.

[127] K. M. Walter, M. Engram, C. R. Duguay, M. O. Jeffries, and F. Chapin, "The potential use of synthetic aperture radar for estimating methane ebullition from Arctic lakes," *JAWRA J. Amer. Water Resour. Assoc.*, vol. 44, no. 2, pp. 305–315, 2008.

[128] G. Pointner, A. Bartsch, Y. A. Dvornikov, and A. V. Kouraev, "Mapping potential signs of gas emissions in ice of Lake Neyto, Yamal, Russia, using synthetic aperture radar and multispectral remote sensing data," *Cryosphere*, vol. 15, pp. 1907–1929, Apr. 2021.

[129] M. Engram and K. W. Anthony, "Synthetic aperture radar (SAR) detects large gas seeps in Alaska lakes," *Environ. Res. Lett.*, vol. 19, Mar. 2024, Art. no. 044034.

[130] M. Kern et al., "The copernicus polar ice and snow topography altimeter (CRISTAL) high-priority candidate mission," *Cryosphere*, vol. 14, pp. 2235–2251, Jul. 2020.

[131] M. W. J. Davidson and R. Furnell, "Rose-l: Copernicus L-band SAR mission," in *Proc. IEEE Int. Geosci. Remote Sens. Symp.*, Jul. 2021, pp. 872–873.

[132] B. Koetz et al., "High spatio- temporal resolution land surface temperature mission - A copernicus candidate mission in support of agricultural monitoring," in *Proc. IEEE Int. Geosci. Remote Sens. Symp.*, Jul. 2018, pp. 8160–8162.

[133] M. C. Korver, B. Lehner, J. A. Cardille, and L. Carrea, "Surface water temperature observations and ice phenology estimations for 1.4 million lakes globally," *Remote Sens. Environ.*, vol. 308, Jul. 2024, Art. no. 114164.

[134] M. Rast, J. Nieke, J. Adams, C. Isola, and F. Gascon, "Copernicus hyperspectral imaging mission for the environment (CHIME)," in *Proc. IEEE Int. Geosci. Remote Sens. Symp.*, Jul. 2021, pp. 157–159.

[135] A. Beamish et al., "Recent trends and remaining challenges for optical remote sensing of arctic Tundra vegetation: A review and outlook," *Remote Sens. Environ.*, vol. 246, Sep. 2020, Art. no. 111872.

[136] B. Sierk et al., "The copernicus CO_2M mission for monitoring anthropogenic carbon dioxide emissions from space," in *Proc. Int. Conf. Space Opt.*, Jun. 2021, Art. no. 118523M.

[137] S. Noël et al., "Greenhouse gas retrievals for the CO_2M mission using the focal method: First performance estimates," *Atmos. Meas. Techn.*, vol. 17, pp. 2317–2334, Apr. 2024.

[138] M. J. Unwin et al., "An introduction to the HydroGNSS GNSS reflectometry remote sensing mission," *IEEE J. Sel. Topics Appl. Earth Observ. Remote Sens.*, vol. 14, pp. 6987–6999, 2021.

[139] D. Comite, L. Cenci, A. Colliander, and N. Pierdicca, "Monitoring freeze-thaw state by means of GNSS reflectometry: An analysis of TechDemoSat-1 data," *IEEE J. Sel. Topics Appl. Earth Observ. Remote Sens.*, vol. 13, pp. 2996–3005, 2020.

[140] K. Rautiainen, D. Comite, J. Cohen, E. Cardellach, M. Unwin, and N. Pierdicca, "Freeze–thaw detection over high-latitude regions by means of GNSS-R data," *IEEE Trans. Geosci. Remote Sens.*, vol. 60, 2022, Art. no. 4302713.

[141] C. Gerlein-Safdi, A. A. Bloom, G. Plant, E. A. Kort, and C. S. Ruf, "Improving representation of tropical wetland methane emissions with Cygnss inundation maps," *Glob. Biogeochemical Cycles*, vol. 35, Dec. 2021, Art. no. e2020GB006890.

[142] P. Lopez-Dekker et al., "The harmony mission: End of phase-0 science overview," in *Proc. IEEE Int. Geosci. Remote Sens. Symp.*, Jul. 2021, pp. 7752–7755.

[143] A. Kääb et al., "Potential of the bi-static SAR satellite companion mission harmony for land-ice observations," *Remote Sens.*, vol. 16, Aug. 2024, Art. no. 2918.

[144] A. G. Lewkowicz and R. G. Way, "Extremes of summer climate trigger thousands of thermokarst landslides in a High Arctic environment," *Nature Commun.*, vol. 10, Apr. 2019, Art. no. 1329.

[145] S. V. Kokelj et al., "Thaw-driven mass wasting couples slopes with downstream systems, and effects propagate through Arctic drainage networks," *Cryosphere*, vol. 15, pp. 3059–3081, Jul. 2021.

[146] M. Schneider et al., "Synergetic use of IASI profile and Tropomi total-column level 2 methane retrieval products," *Atmos. Meas. Techn.*, vol. 15, pp. 4339–4371, Jul. 2022.

[147] J. Day et al., "Development of the TANGO carbon instrument for greenhouse gas detection," *Proc. SPIE*, vol. 12735, Oct. 2023, Art. no. 127350I.

[148] S. Nikolov, C. Wührer, C. Kühl, M. Bode, W. Hupfer, and S. Lucarelli, "Merlin: Design of an IPDA LiDAR instrument," *CEAS Space J.*, vol. 11, pp. 437–457, Aug. 2019.

[149] P. Bousquet et al., "Error budget of the methane remote lidar mission and its impact on the uncertainties of the global methane budget," *J. Geophysical Res.: Atmos.*, vol. 123, pp. 11,766–11,785, Oct. 2018.

[150] M. Goldberg, "The joint polar satellite system overview," in *Proc. IEEE Int. Geosci. Remote Sens. Symp.*, Jul. 2018, pp. 1581–1584.

[151] L. Zhou, M. Divakarla, and X. Liu, "An overview of the joint polar satellite system (JPSS) science data product calibration and validation," *Remote Sens.*, vol. 8, Feb. 2016, Art. no. 139.

[152] A. Das, R. Kumar, and P. Rosen, "Nisar mission overview and updates on ISRO science plan," in *Proc. IEEE Int. India Geosci. Remote Sens. Symp.*, Dec. 2021, pp. 269–272.

[153] P. A. Rosen and R. Kumar, "NASA-ISRO SAR (NISAR) mission status," in *Proc. IEEE Radar Conf.*, May 2021, pp. 1–6.

[154] GCOS, "The 2022 GCOS implementation plan," World Meteorological Org., Geneva, Switzerland, Tech. Rep. GCOS-244, 2022.

[155] GCOS, "The 2022 GCOS ECVs requirements," World Meteorological Org., Geneva, Switzerland, Tech. Rep. GCOS-245, 2022.
[156] W. Dobiński, "Permafrost active layer," *Earth- Sci. Rev.*, vol. 208, Sep. 2020, Art. no. 103301.
[157] K. Wu et al., "Evaluating the ability of the pre-launch Tansat-2 satellite to quantify urban CO_2 emissions," *Remote Sens.*, vol. 15, Oct. 2023, Art. no. 4904.
[158] Y. Yoshida et al., "Retrieval algorithm for CO_2 and CH_4 column abundances from short-wavelength infrared spectral observations by the greenhouse gases observing satellite," *Atmos. Meas. Techn.*, vol. 4, pp. 717–734, Apr. 2011.
[159] M. N. Deeter et al., "The mopitt version 6 product: Algorithm enhancements and validation," *Atmos. Meas. Techn.*, vol. 7, pp. 3623–3632, Nov. 2014.
[160] D. Fu et al., "High-resolution tropospheric carbon monoxide profiles retrieved from Cris and Tropomi," *Atmos. Meas. Techn.*, vol. 9, pp. 2567–2579, Jun. 2016.
[161] J. Landgraf and O. P. Hasekamp, "Retrieval of tropospheric ozone: The synergistic use of thermal infrared emission and ultraviolet reflectivity measurements from space," *J. Geophysical Res.: Atmos.*, vol. 112, Apr. 2007, Art. no. D08310.
[162] E. Malina et al., "Joint spectral retrievals of ozone with Suomi NPP CrIS augmented by S5P/TROPOMI," *Atmos. Meas. Tech.*, vol. 17, pp. 5341–5371, Sep. 2024, doi: 10.5194/amt-17-5341-2024.
[163] E. Gorman et al., "The NASA plankton, aerosol, cloud, ocean ecosystem (pace) mission: An emerging era of global, hyperspectral earth system remote sensing," *Proc. SPIE*, vol. 11151, Oct. 2019, Art. no. 111510G.
[164] E. N. Stavros et al., "Designing an observing system to study the surface biology and geology (SBG) of the earth in the 2020 S," *J. Geophysical Res.: Biogeosciences*, vol. 128, Jan. 2023, Art. no. e2021JG006471.
[165] B. A. Gay et al., "Investigating high-latitude permafrost carbon dynamics with artificial intelligence and earth system data assimilation," PhD Thesis, Dec. 2023.
[166] National Research Council, *Opportunities to use remote sensing in understanding permafrost and related ecological characteristics: Report of a workshop*. Washington, DC, USA: National Academy Press, Jun. 2014.
[167] L. Buffet, P. Gamet, P. Maisongrande, C. Salcedo, and P. Crebassol, "The TIR instrument on Trishna satellite: A precursor of high resolution observation missions in the thermal infrared domain," in *Proc. Int. Conf. Space Opt.*, Jun. 2021, Art. no. 118520Q.
[168] J.-L. Roujean et al., "TRISHNA: An Indo-French space mission to study the thermography of the earth at fine spatio-temporal resolution," in *Proc. IEEE Int. India Geosci. Remote Sens. Symp.*, Dec. 2021, pp. 49–52.
[169] R. R. Basilio, S. J. Hook, S. Zoffoli, and M. F. Buongiorno, "Surface biology and geology (SBG) thermal infrared (TIR) free -flyer concept," in *Proc. IEEE Aerosp. Conf.*, Mar. 2022, pp. 1–9.
[170] A. K. Thorpe et al., "Attribution of individual methane and carbon dioxide emission sources using emit observations from space," *Sci. Adv.*, vol. 9, Nov. 2023, Art. no. eadh2391.

Annett Bartsch (Member, IEEE) received the Diploma (M.Sc.) degree from the Friedrich-Schiller University of Jena, Jena, Germany, in 2000, and the Ph.D. degree from The University of Reading, Reading, U.K., in 2004, both in geography.

From 2003 to 2012, she has been with the Vienna University of Technology, Vienna, Austria, and received her venia docendi in applied remote sensing in 2011. She has been visting professor at the University of Salzburg, Austria, from 2012 to 2013 and substitute professor at LMU Munich, Germany, from 2013 to 2014. From 2014 to 2016, she was the head of the Climate Change Impacts section, Zentralanstalt für Meteorologie und Geodynamik, Vienna. Since 2017, she is managing director of the b.geos GmbH, Korneuburg, Austria. She focuses on the application of satellite data at high latitudes related to land surface hydrology and for interdisciplinary studies. Her research interests include active microwave remote sensing techniques for analyses of frozen ground, wetlands, lakes, and snow.

Bradley A. Gay received the bachelor of science degree in biology from the University of Nebraska, Lincoln, NE, USA, in 2010, the M.Sc. degree in environmental sciences and policy from Johns Hopkins University, Baltimore, MD, USA, in 2012, and the Ph.D. degree in Earth systems and geoinformation sciences from George Mason University, Fairfax, VA, USA, in 2023.

He is a NASA Postdoctoral Program Fellow with the Carbon Cycle and Ecosystems Group, Jet Propulsion Laboratory, California Institute of Technology, Pasadena, CA, USA. His Ph.D. research focused on high-latitude permafrost carbon dynamics using artificial intelligence and Earth system data assimilation. He collaborates with leading scientists across NASA, ESA, and other research institutions to advance Arctic science and inform climate policy. His work leverages remote sensing technologies, process-based models, quantum mechanics, and AI-driven frameworks to investigate freeze-thaw dynamics and the permafrost carbon feedback while quantifying climate-driven ecosystem changes across the Arctic. His research interests include in situ measurements, airborne remote sensing, and satellite observations to develop innovative methodologies for monitoring the Cryosphere.

Dirk Schüttemeyer received the Diploma degree in meteorology from Bonn University, Bonn, Germany, in 2000 and the Ph.D. degree in meteorology from Wageningen University, Wageningen, The Netherlands in 2005.

He was with Wageningen University, University München, Munich, Germany, and Bonn University before joining the European Space Agency (ESA) as Campaign Scientist. He is currently the Mission Scientist for the Arctic Weather Satellite and MicroWave Sounder (MWS) on MetOp-SG. His current research interests include active and passive remote sensing, land-atmosphere interaction, data assimilation, and weather forecasting.

Edward Malina received the masters (M.Eng.) degree in aerospace engineering from the University of Sheffield, Sheffield, U.K., and Virginia Tech, Blacksburg, VA, USA, in 2010, and the Ph.D. degree in atmospheric physics from University College London, London, U.K., in 2018.

He is currently an Atmospheric Scientist with the European Space Agency (ESA) Centre for Earth Observation (ESRIN), Frascati, Italy. His main responsibilities include supporting the European scientific community in undertaking advanced atmospheric research using ESA Earth observation missions.

Kimberley Miner received the Ph.D. degree in Earth and climate sciences from the University of Maine, Orono, ME, USA, in 2018.

She is currently a Scientist and Program Manager with the NASA Jet Propulsion Lab, La Ca Flintridge, CA, USA. Before coming to NASA, she worked on climate security with the Department of Defense in DC and holds a research Professorship with the University of Maine and Virginia Tech. She is also writing a book on how younger generations can plan for climate change, to be released in 2024.

Guido Grosse received the Diploma (M.Sc.) degree in geology from the Technical University and Mining Academy Freiberg (TUBA), Freiberg, Germany, in 2001, and the Dr. rer. nat. (Ph.D.) degree in geosciences from the University of Potsdam, Potsdam, Germany, in 2005.

He became Postdoc and then Research Assistant Professor with the Geophysical Institute of the University of Alaska Fairbanks, USA, in 2006 and 2009, respectively. In 2013, he received an ERC Starting Grant and started at the Alfred Wegener Institute (AWI) Helmholtz Centre for Polar and Marine Research in Germany. Since 2016, he has been a Full Professor on Permafrost in the Earth System jointly appointed by AWI and the University of Potsdam and became the Head of the Permafrost Research Section, AWI. His research interests include a combination of field studies and remote sensing of landscape dynamics across broad spatial and temporal scales, hydrology, carbon cycling, and the impacts of climate change in Arctic permafrost regions.

Andreas Fix received the Diploma degree in physics from University of Hannover, Hanover, Germany, in 1989 and the Dr. rer. nat. (Ph.D.) degree in physics from the University of Kaiserslautern, Kaiserslautern, Germany in 1994, with a focus on laser physics and nonlinear optics.

In 1995, he joined the Institute of Atmospheric Physics of German Aerospace Center (DLR) first as a Postdoc and later as a Research Associate. In 2000, he was Visiting Scientist with National Oceanic and Atmospheric Administration (NOAA), Boulder, CO, USA. Since 2018, he has been the Head of the Lidar Department, DLR Institute of Atmospheric Physics.

Dr. Fix participated in numerous airborne field campaigns, both national and international, and developed and operated various lidar systems for this purpose. Currently, he serves as a Member for the Scientific Advisory Group (SAG) of the joint French-German climate initiative (MERLIN) and acts as the lead scientist for the CoMet series of airborne missions for monitoring greenhouse gases onboard the German research aircraft HALO.

Johanna Tamminen received the Ph.D. degree in applied mathematics from the University of Helsinki, Helsinki, Finland, in 2004.

She joined the Finnish Meteorological Institute (FMI) in 1992 to develop computational methods and uncertainty quantification for satellite remote sensing applications and has worked there ever since. Over the years, her interests have widened from remote sensing of ozone to air quality, greenhouse gases, emissions and more generally to climate. Currently, she is a Research Professor with the FMI and leading the FMI's Earth Observation Research Unit.

Dr. Tamminen is the Vice Director of Research council of Finland funded Centre of Excellence in Inverse Modeling and Imaging (2018–2025), co-PI of recently launched National research Flagship on Advanced Mathematics for Sensing Imaging and Modeling, and Co-PI of Ozone Monitoring Instrument on-board EOS-Aura satellite.

Hartmut Bösch received the Diploma (M.Sc.) and the Ph.D. degrees in physics and astronomy from the University of Heidelberg, Heidelberg, Germany, in 1998 and 2002, respectively.

He then became Postdoc and a Scientist with the NASA Jet Propulsion Laboratory (JPL) where he worked on the NASA Orbiting Carbon Observatory (OCO) mission. He joined the University of Leicester, Leicester, U.K., in 2007 as a Research Fellow and became a Lecturer in 2012, followed by promotion to Reader in 2013 and to Professor in 2017. Between 2015 and 2022, he was the Head of the Earth Observation Science Group, University of Leicester and a Divisional Director of the National Centre for Earth Observation (NCEO). In 2022, he joined the Institute of Environmental Physics, University of Bremen, Bremen, Germany, as a Professor in atmospheric physics and chemistry. His research interests include the use of satellite remote sensing methods to diagnose and understand the carbon and methane exchange between the atmosphere and surface.

Robert J. Parker received the Ph.D. degree in atmospheric physics from the University of Leicester, Leicester, U.K., in 2009.

He subsequently worked as a Postdoctoral Research Associate for the U.K. National Centre for Earth Observation focused on satellite remote sensing of atmospheric methane. In 2015, he was awarded a European Space Agency Living Planet Fellowship where he led work on evaluation of land surface model methane emissions, including within the U.K. Earth System Model. He was recently (2024) appointed as a Lecturer in Earth observation with the School of Physics and Astronomy, University of Leicester.

Dr. Parker was awarded a UKRI Future Leaders Fellowship, in which he is leading work to develop a tropical wetland methane digital twin.

Kimmo Rautiainen received the D.Sc. (Tech.) degree in geoinformatics from the School of Engineering, Aalto University, Espoo, Finland, in 2018.

He was a Research Scientist with the Laboratory of Space Technology, Helsinki University of Technology (TKK), Espoo, where he focused on microwave radiometer systems with an emphasis on interferometric radiometers. Since 2010, he has been with Finnish Meteorological Institute (FMI), Helsinki, Finland. He is a Senior Scientist with the Earth Observation Research, specializing in the development of retrieval algorithms for passive microwave remote sensing, with a focus on cryosphere applications.

Josh Hashemi received the Ph.D. degree in ecology from the University of California, Davis, Davis, CA, USA, and San Diego State University, San Diego, CA, USA, in 2022.

He is currently a Postdoctoral Scientist with the Permafrost Research Section, Alfred Wegener Institute Helmholtz Centre for Polar and Marine Research (AWI), Bremerhaven, Germany. His work combines field observations and computational methods to study permafrost systems and their role in the global climate system. His research interests include Arctic landscape ecology, wetland morphology, remote sensing, and the application of machine learning to spatial modeling.

Charles E. Miller received the B.S. degree in chemistry and history from Duke University, Durham, NC, USA, in 1986 and the Ph.D. degree in chemical physics from the University of California, Berkeley, Berkeley, CA, USA, in 1991.

He was a Welch Postdoctoral Fellow with Rice University and a National Research Council Fellow with the NASA Jet Propulsion Laboratory (JPL). He is a Principal Scientist with JPL and a Visiting Associate in environmental science and engineering with the California Institute of Technology, Pasadena, CA, USA. He has over 25 years of experience leading satellite and suborbital projects for NASA Earth Sciences. He currently serves as NASA Lead for the NASA-ESA Arctic Methane and Permafrost Challenge (AMPAC) and Deputy Science Lead for NASA's Arctic-Boreal Vulnerability Experiment (ABoVE). His research interests include carbon cycle science, Arctic system science, atmospheric photochemistry, and molecular spectroscopy, with an emphasis on developing innovative spectroscopic solutions for satellite and airborne remote sensing of greenhouse gases and anthropogenic emissions.